ZEOLITIC-IMIDAZOLATE FRAMEWORK ZIF-67 MEMBRANES EXHIBITING HIGH PROPYLENE/PROPANE SEPARATION PERFORMANCES

A Thesis

by

CHEN YU

Submitted to the Office of Graduate and Professional Studies of
Texas A&M University
in partial fulfillment of the requirements for the degree of

MASTER OF SCIENCE

Chair of Committee,	Hae-Kwon Jeong
Co-Chair of Committee,	Hong-Cai Joe Zhou
Committee Member,	Hung-Jen Wu
Head of Department,	M. Nazmul Karim

August 2019

Major Subject: Chemical Engineering

ABSTRACT

Propylene/propane membrane based separation is one of the most challenging tasks in modern chemical industry due to their similar chemical and physical properties. Current most well-developed method of separating propylene/propane is by applying multi-column distillation system which is extremely energy intensive and costly. Membrane-based separation method have provided a feasible way to solve this long existing problem but the performances (selectivity and permeance) of current most widely used polymeric membranes are still not satisfying.

Zeolitic imidazolate framework (ZIFs), a kind of nanoporous material based on zeolitic topologies, has shown impressive potential in hydrocarbon gas separation attribute to its tunable structure and good thermal and chemical stability. Among all ZIF family members, ZIF-8, a promising candidate with effective aperture size of 4.0 Å has been proved to possess unprecedentedly high propylene/propane separation performance, well above the traditional polymeric upper limit. Its cobalt-substituted isostructural version, ZIF-67, have been predicted to have smaller effective aperture size (~3.9 Å) and therefore much better selectivity while relatively maintaining the permeance. However, syntheses of high-quality phase-pure ZIF-67 was challenging and no phase-pure ZIF-67 membrane have ever been reported of any propylene/propane selectivity. Meanwhile, considering the high unit area cost of ZIF membrane, ultra-thin membrane with desired performance is highly demanded to improve the productivity and production intensity.

In this research, I would like to demonstrate the successful syntheses of defect-free, ultrathin phase-pure ZIF-67 (thickness: 300 – 500 nm) membranes as well as ZIF-8 membranes via a novel seeding method named combined seeding. This combined seeding method consists of

well-developed microwave-assisted seeding and electrophoretic nuclei assembly for crystallization of highly intergrown thin-films (ENACT) as the seeding procedure followed by a solvothermal secondary growth. The as-synthesized ZIF-67 showed a decent propylene/propane separation factor of 67 and a propylene permeance of ~ 80 GPUs. With an additional tertiary growth, the separation factor was increased to a record-high 298 with a propylene permeance of 30 GPUs. Furthermore, when the membranes were subjected upon post-synthetic ligand exchange (PSLE), the propylene permeance was enhanced to ~298 GPUs with a propylene/propane separation factor of 19. It should be noted that this is the first reported case of phase-pure ZIF-67 membranes showing propylene/propane separation.

ACKNOWLEDGEMENTS

First of all, I would like to thank my advisor, Dr. Jeong, for his patience and his professional suggestions that helped me so much during my graduate research and study. His dignity and preciseness toward science affect me in every way.

I would also like to thank all the committee members, Dr. Zhou and Dr. Wu for their guidance and support throughout the research and preparation of my thesis. Thanks for their time and their understanding.

I'm grateful for my colleagues as well. Thanks to Jingze Sun, he helped me and taught me so much in preparing my paper. It has been a great honor to work with him. Thanks to Dr. Kie Yong Cho's help, he taught me a lot about basic principles and innovative way to think problems. Also, I'm grateful for my friend's companionship, Febrian, rezi, Moonjoo and Sunghwan. I really enjoyed my life when they are around me and I sincerely appreciate those who supported me for I could not have achieved all this without them.

At last, I want to express my gratitude to my beloved family and my girlfriend for their understanding and love. The warmth from thousand miles away comforted my heart and brought me strength and courage.

CONTRIBUTORS AND FUNDING SOURCES

Contributors

This work was supervised by a thesis committee consisting of Dr. Hae-Kwon Jeong which is also my advisor and Dr. Hung-Jen Wu of the Department Chemical Engineering and Dr. Hong-Cai Joe Zhou of the Department of Chemistry.

The data analyzed for section 4.3 and 5.2.2 was provided by Dr. Kie-Yong Cho of the Department of Chemical Engineering.

All other work conducted for the thesis was completed by the student independently.

Funding Sources

There are no outside funding contributions to acknowledge related to the research and compilation of this document.

TABLE OF CONTENTS

Page

LIST OF FIGURES

Page

LIST OF TABLES

Page

CHAPTER I

INTRODUCTION

Propylene is a kind of strongly desired chemical mainly used for production of polypropylene, acrylonitrile (ACN) and acrylic acid etc. The main source of propylene is from petroleum cracking and natural gas processing together with other conversion technologies like dehydrogenation and fluid catalytic cracking (FCC). No matter which method we apply, it requires propylene been separated from propane, a kind of paraffin that always appears as a side product in propylene production. Due to their similar molecular size and chemical property,[1-2] the separation process using traditional methods such as distillation system and physical or chemical absorption[3] is extremely energy intensive. However, membrane-based gas separation method provided an innovative solution to this long-existing problem.

There are multiple potential candidates been reported for propylene/propane separation membrane material in recent years, including but not limited to, polymeric membranes,[4] molecule sieves membranes[5] and mixed matrix membranes.[6] To meet the production demands and improve the most important criteria, permeability and selectivity, the selection of membrane material need to meet certain requirements. It has to be thin, scalable, stable under production condition and be able to be packed into high-surface-area modules.[7] Considering the cost and easy access, polymeric membrane is playing a major role in gas separation membrane material. Unfortunately, a minimum propylene selectivity standard of 35 or above is required in order to be commercially attractive.

The limitation of polymeric membrane duration and its relatively low selectivity is impeding it from massive application. As a result, high performance material is urgently demanded.

Metal-organic frameworks (MOFs),[8-9] attribute to their tunable pore size and high porosity therefore high specific surface area,[10] have provided a feasible membrane-based, energy-saving, propylene propane separation solution. As a sub-class of MOFs, zeolitic imidazolate framework,[11-12] a kind of nanoporous material based on zeolitic topologies, consist of transition metal nodes and organic linkers, have shown impressive performance in gas separation well above traditional polymer upper bound.[13] With better thermal and chemical stabilities as compared to other MOFs and robust synthesis protocols,[14] ZIF material has drawn people's strong attention in gas separation application. As the most well investigated member in ZIF family, ZIF-8 [11] has been thoroughly studied. Combined by coordination bond between zinc ions and 2-methylimidazoles, ZIF-8 has effective aperture size of 4.0–4.2 Å [15] considering its flapping motion of the linker[16] which provide perfect fitness for propylene/propane separation. ZIF-8 was then successfully synthesized into membrane [12] and showed C2/C3 separation performance [13].

The best ZIF-8 membrane was synthesized on alumina support with astonishing propylene/propane selectivity factor of ~200,[17] whereas the permeance of propylene, in another word, productivity, was still far from industrial practical needs. To improve the productivity, the most straight forward way is to decrease the membrane thickness but considering the difficulties of controlling the grain boundary structure and the surface roughness of the support after downsizing, ultra-thin ZIF-8 membrane with ideal selectivity is not that easy to synthesize. In the

meantime, ZIF-67 has shown potentially preeminent performance superior than ZIF-8 in propylene-propane separation.[18-19] In general, ZIF-67 is Co-substituted ZIF-8, due to higher angle of Co−N and N−Co−N bond than Zn and the K constant of the harmonic angle in Co-ZIF is 3 times higher than Zn-ZIF, ZIF-67 has more rigid structure with a smaller oscillation of the gate-opening thereby smaller aperture size.[19] Until now, multiple attempts in synthesizing ultra-thin phase-pure ZIF-67 membrane with high propylene/propane separation performance have been made yet none of them have shown promising result. Either by heteroepitaxial growth[20] or by introducing other chemical precursors, [21] the resulting membranes were always grown into loosely packed structure with micro-level thickness however no selectivity. Beside, impurities have been observed when synthesizing ZIF-67 directly on supports using current processing techniques. Therefore, it's necessary to develop a new kind of synthesize method with robust protocol that can overcome those aforementioned problems.

In the aim of fabricating ultra-thin, phase-pure ZIF-67 membrane with ideal propylene/propane separation performance, this research introduces a novel facile seeding method (named combined seeding) for ultrathin phase-pure ZIF-67 membrane synthesis on utilitarian porous α-Al_2O_3 support. Our combined seeding method could reduce the size of seeding crystals to ~ 20 nm by conjoining microwave seeding (using TEA) with electrophoresis deposition seeding technique (ENACT), which can not only smooth the surface of the support but also provide surface anchoring for the membrane. After the solvothermal secondary growth, our membrane showed an average propylene/propane separation factor of ~ 67 with an average propylene permeance of ~80

GPUs and a thickness of 300-500 nm, which is the first phase-pure ZIF-67 membranes showing propylene/propane separation. In addition, the selectivity and the propylene permeance could be further enhanced to ~ 292 and ~ 80 GPUs by tertiary growth and post-synthetic linker exchange (hereafter, PSLE). This combined seeding method was also proved to be successful in synthesizing ultrathin ZIF-8 membranes.

The thesis is comprised of several chapters. The following chapter II provides general background and review of the propylene market status and previous propylene/propane separation method together with current ZIF-8 and ZIF-67 research progress. Our experiment section is presented in chapter III, explaining our synthesis method and characterization method. Chapter IV contains our detailed results and discussion, ENACT seeding optimization process is also included. To further improve our membrane performances, post synthetic treatments are included in chapter IV, which is basically about tertiary growth and PSLE process and results. The remaining problem of this combined-seeding method and other application will be discussed in chapter V together with our future suggestions and future plans on related topic.

CHAPTER II

BACKGROUNDS AND OVERVIEW

2.1 Propylene Industry Overview

2.1.1 Propylene market status and production

Polypropylene (PP) is one of the most important polymers in current plastic industry due to its outstanding mechanical and chemical properties, its wide application in automobile, packaging, electronics and aerospace industry have secured its position in polymer market. Considering current increasing polymer consumption and growing need for relative downstream chemical products, the momentum of the polypropylene industry is further anticipated to massive growth over a long time period. Correspondingly, propylene, the monomer of polypropylene, is facing an escalating demand for polypropylene production.

As a matter of fact, propylene is one of the largest consumed and the oldest petrochemical feedstock across the globe, employed as it was in the early processes to isopropanol. Except for polypropylene, it is also widely used for the production of propylene oxide, acrylic acid and cumene etc. As we can see from Figure 2.1, in the year of 2001, about 61.6% of the propylene produced is used for the production of polypropylene while 8% fractions of the total are consumed for propylene Oxide production, the preparation of the “oxo-alcohols,” and for other application took up 8.4% and the rest 11.5%.

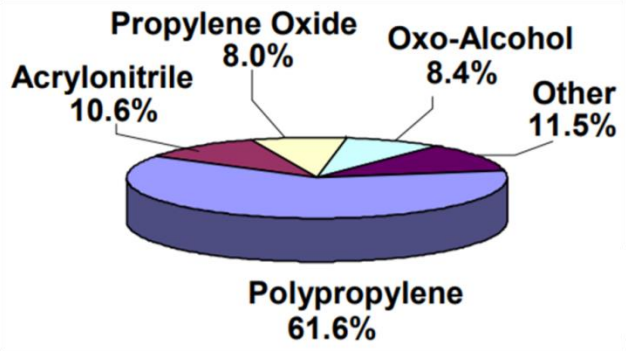

Figure 2.1 US propylene consumption distribution plot. The growing need for polypropylene is the main driving force for propylene industry. [22] Copyright 2001, ExxonMobil.

By far, the production of polypropylene is booming in size and scale, it is now the largest volume plastic in the world. To support its extensive growth, modern polypropylene units typically require about 300 thousand metric tons per year (300 kta) of propylene per train for feedstock.[22] Since the crude oil price these years is continuing favorable for petrochemical industry and the strong developing trend in Asia Pacific area, the propylene market is optimistic in general. From Figure 2.2, the trend of US propylene market, the annual growth of propylene production is about 6%/yr, and the portion of polypropylene is anticipated to take a larger part. However, the growing rate of polypropylene is well beyond current propylene supply rate, which means, the supply is facing some severe restraints. Therefore, propylene productivity needs to be increased to a much higher level.

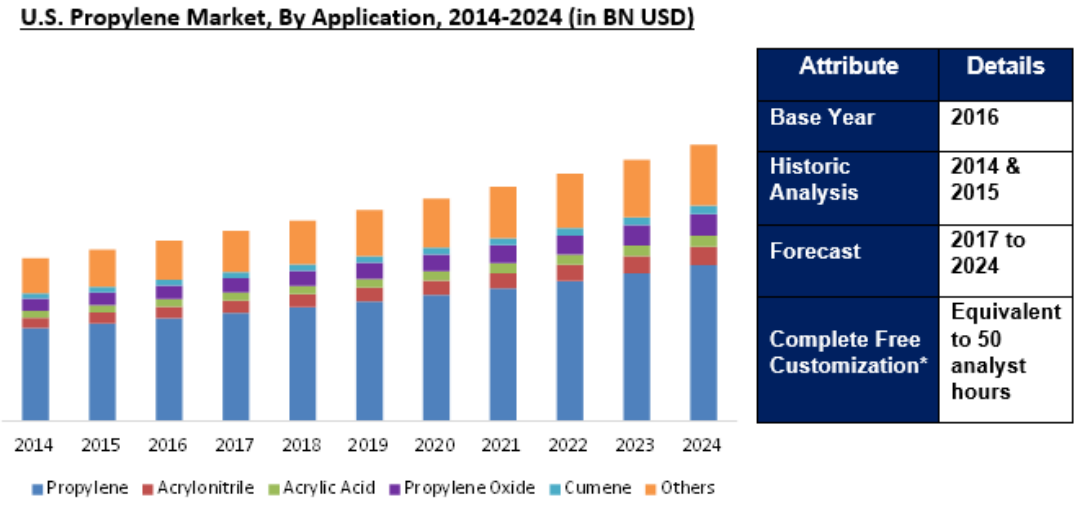

Figure 2.2 US propylene market trend and forecast. Copyright 2017, AMERI RESEARCH INC.

At present, most of the world's propylene comes from steam cracker by the need for ethylene, where propylene in this circumstance, plays a role as co-product,[23] however its low productivity can no longer keep up with the growing pace of the need. Furthermore, co-product propylene production from steam cracking is largely determined by ethane feed, which produces little propylene.[24] As a result, there is an increasing need for propylene from other sources. Except from naphtha or liquefied petroleum gas cracking process, the second largest amount of propylene comes from refineries as a byproduct from fluidized catalytic cracker (FCC) units that are operated for gasoline production.[25]

Those two sources mentioned above used to supply all of the world's propylene need but with the increasing of the cost from ethylene production, enterprises are seeking new cost-efficient way for propylene production which is so called on-purpose propylene (OPP) technologies.[24-25]

Currently the most widely applied OPP technologies are propane dehydrogenation (propane is catalytically dehydrogenated to give propylene and hydrogen) and olefin metathesis (ethylene and 2-butene are catalytically metathesized to give propylene). Propane dehydrogenation is gaining more interests compared to the other method giving its relatively low cost, a rising problem in separating propylene/propane gas pair in order to increase the propylene yield is becoming a major concern. Even though the traditional way of propylene production is still playing a major role, with the sharply rising trend of the need and the increasing price of raw materials, OPP has been accepted by plastic industry in recent years.

2.1.2 Propylene/propane Separation method

By the year of 1991, the estimated annual energy consumption for olefin/paraffin separation already exceed 0.12 Quads (1 Quad=10^{15} BTU) and the corresponding capital cost also spectacular.[3] With the declining of the natural gas supply in North America, the major source of olefin production will be from crude oil cracking which requires much cost-efficient technologies with good thermal and physical properties that can stand harsh production condition.

The most typical method for separation is traditional distillation system. It requires streams to contain high quantities of olefin, so it's only attractive for large refinery catalytic crackers and high-capacity ethylene crackers. Regarding the similar boiling point of propylene (-47.6 ^{o}C) and propane (-42 ^{o}C), the number of trays to achieve desired purity level is typically over 200.[26-27] Since the processes always involve phase-change, the energy cost is massive. An alternative is by

physical adsorption or chemical absorption, since physical adsorption can indeed lower the energy consumption however it requires complicated desorption and regeneration cycles and its capital cost is typically higher than comparable distillation process so it has never been widely accepted.[3] Chemical absorption on the other hand, requires frequent inspection and maintenance for contamination problems, its low olefin loadings also hindered it from further application. Recent years, hydrocarbon separation through membrane-based method seems to be a feasible solution to the above mentioned concerns.

Membrane-based separation method, compared to traditional technologies, does not involve phase change or any frequent maintenance therefore it's relatively easy to operate and process option. Since the membrane approach requires the use of relatively simple and non-harmful materials, it's also favorable for massive production.[28] The most promising candidates so far are polymeric, inorganic and facilitated transport membranes.[26] Regardless of its speed and selectivity, facilitated membrane are very vulnerable toward osmotic forces and inverted micelles, let along its carrier poisoning issue. As a result, the facilitated membrane was not considered practical.[29] In the previous section, we have discussed the trade-off relationship between permeability and selectivity of polymeric membranes, the polymer upper bound must be surpassed in order to meet the demands. Therefore, more effort has been devoted to inorganic micro porous membranes like ZIFs, carbon molecular sieve and mixed matrix membranes. Among all these candidates, much recent efforts have been devoted to ZIFs development for it has shown impressive versatility. The robustness of ZIFs physical and chemical properties and its ability of

being packed into compact size modules would be beneficial to continuous production without regeneration. Moreover, the versatility of ZIFs structure makes it possible for further modification which allows multi-tasks separation. Therefore, ZIFs have attracted much attention for future membrane material candidate.

2.2 ZIFs

2.2.1 Definition

Metal-organic frameworks (MOFs) [8-9] are a class of microporous crystalline materials typically comprised of inorganic metal cations and multidentate organic linkers. Since the variety of combination of metal nodes and inorganic linkers, the possible structure of MOFs is nearly unlimited.[30] As a sub-class of metal organic frameworks (MOFs), zeolitic-imidazolate frameworks (ZIFs) [11-12], consist of tetrahedral transition metal nodes (Zn,[11-13] Co,[20, 31-32] Cd[33-35]) and imidazole-derived organic linkers. With extended 3D structure, ZIFs have shown permanent porosity and much better thermal and chemical stabilities as compared to other MOFs as well as robust synthesis protocols.[14] The synthesis of ZIFs essentially depends on the coordination ability of the metal centers and organic linkers. By substituting the metal ions and corresponding inorganic linkers, ZIFs have gained much flexibility and controllability toward their adsorption and pore size properties. More than 150 ZIF structures have been reported so far, some of which share the same topology as zeolites considering the fact that the M-Im-M angle in ZIFs is similar to the Si-O-Si

angle in zeolites,[36] while others exhibit crystal structures which are different from zeolites.[37] Some typical topologies are listed in Figure 2.3.

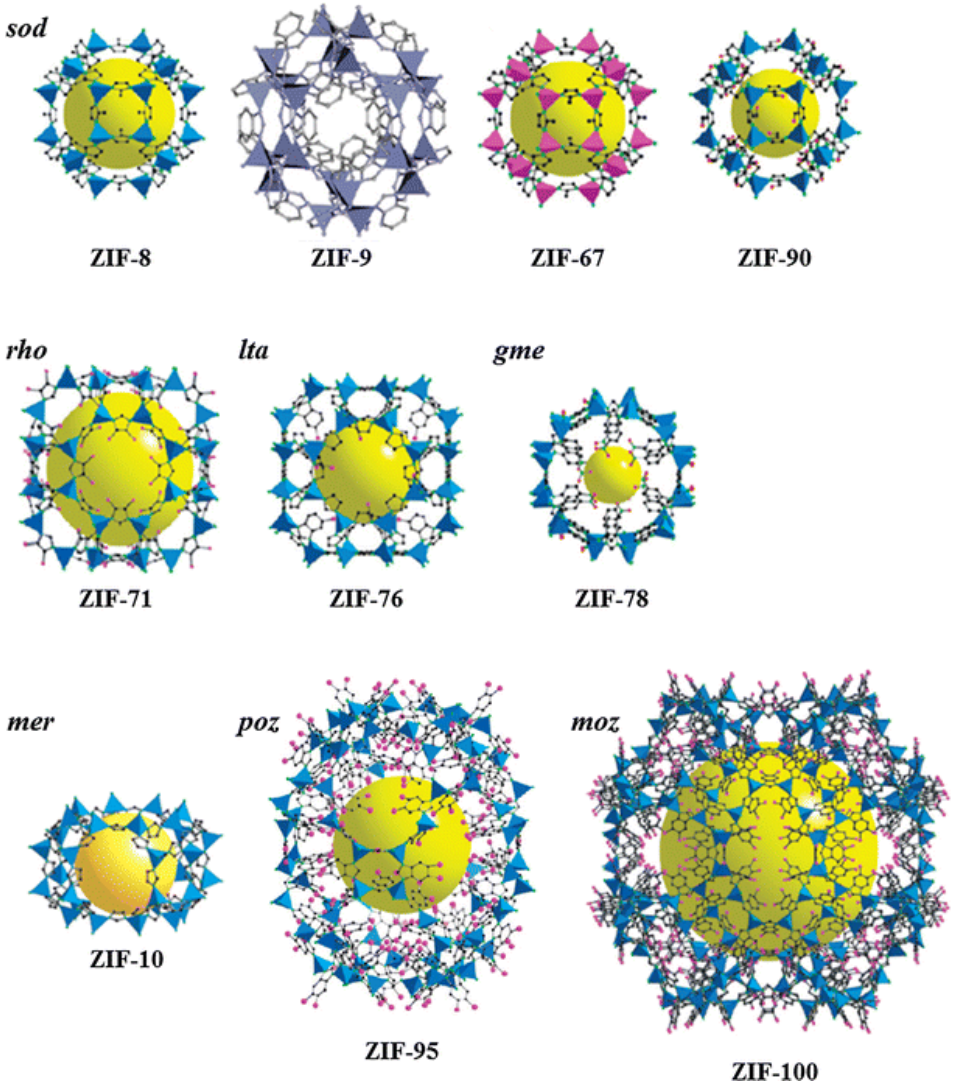

Figure 2.3 Typical ZIF with various topologies. Reproduced with permission.[38] Copyright 2014, Catalysis Surveys from Asia.

Moreover, for the purpose of gas separation, the abundant options for organic linker further allow ZIFs to be customizable for different gas pair separation. By changing the linker with bulkier or smaller imidazole molecule, the oscillation of the gate-opening effect will substantially be enhanced or depressed, detailed principle will be discussed in the following section. The common linker candidates are listed below in Figure 2.4. Attribute to their tunable pore size and high porosity therefore high specific surface area,[10] ZIFs have provided a feasible membrane-based, energy-saving, propylene propane separation solution. It has also attracted tremendous research interest in various applications, including gas storage,[39-40] gas separation,[9, 41-42] , drug deliver,[43-44] catalysis,[45-46] and so on.[47-49]

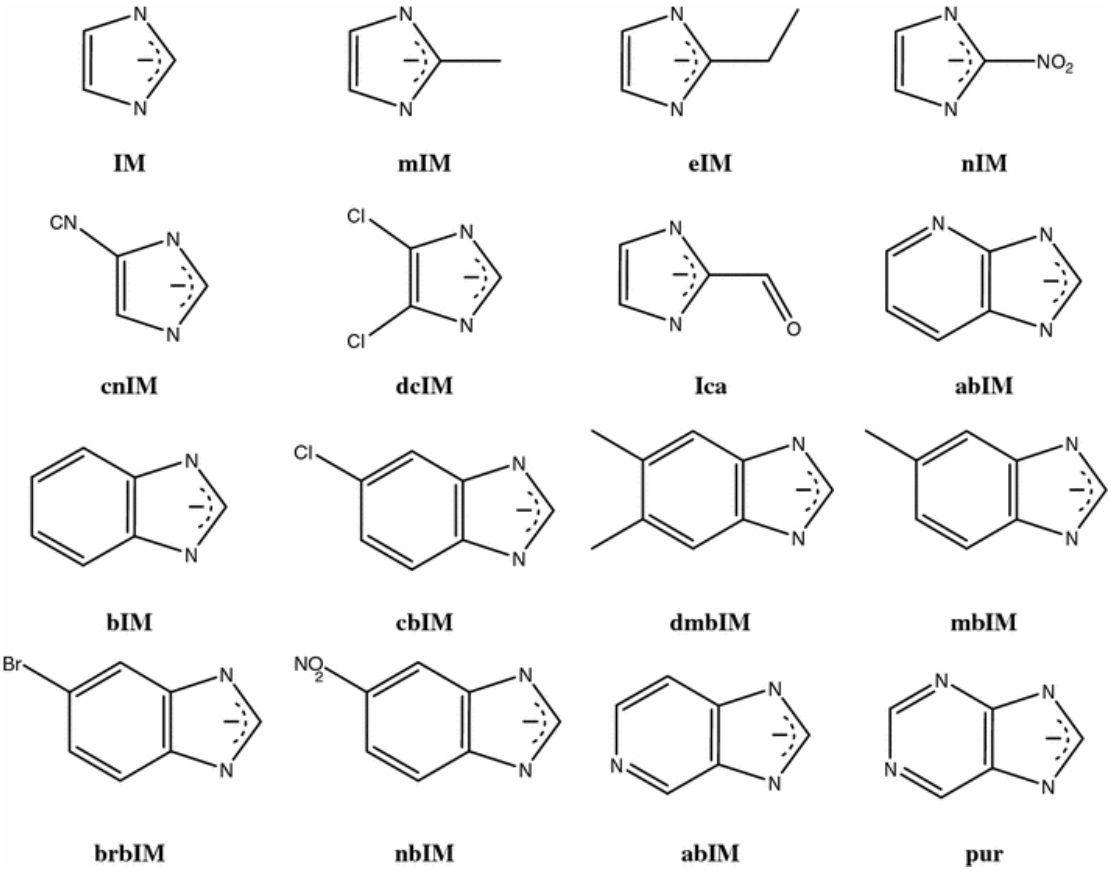

Figure 2.4 Various imidazolate linker candidates used for ZIFs synthesis. Reproduced with permission.[38] Copyright 2014, Catalysis Surveys from Asia.

2.2.2 Application in gas separation

In the last section, we talked about the potential gas separation ability of ZIFs thanks to its gate-opening dynamic behavior. In previous researches, a threshold pressure for ZIFs to uptake and release big molecules was observed,[11] indicating a rotation pattern of the organic linkers in ZIFs. The gate-opening effect of ZIFs was confirmed to be guest molecule induced which means it was triggered by the absorption of certain gas molecule at threshold pressure.[16] By using high-resolution neutron and synchrotron vibrational spectroscopy with *ab initio* density-functional

simulations, Ryder et al. [50]have confirmed the ligand rotational pattern of ZIF-4, ZIF-8 and ZIF-7. Recognized the flapping motion of the linkers in ZIFs, the kinetic diameter of ZIFs aperture size is considerably larger than the crystallographic pore size, leading to an unexpected selectivity of ZIFs materials. Soon, the flexibility of ZIFs has gained much interest in gas separation.

For membrane-based separation, the good nature of ZIFs has been widely studied. Well-intergrown, defect-free ZIF membrane have shown unprecedentedly sharp cut off when applied in hydrocarbon gas separation. Caro et al.[51] have demonstrated the ability of separating H_2/CO_2 of ZIF-7 synthesized by dip-coating process followed by secondary growth on asymmetric alumina disk. Zhiping Lai et al.[13] have successfully separated multiple C2/C3 gas pairs using ZIF-8 membrane synthesized in aqueous solution, the membrane was only 2.5 μm thick with selectivity of propylene/propane around 18. ZIF-69 solvothermal synthesized membrane can work perfectly as CO_2/CO separation candidate.[52] Except for above mentioned results, ZIFs membranes with mixed linker[53] or mixed metal[33] have also been successfully synthesized and shown its enormous potential in various gas pairs separation. Moreover, ZIFs could be further combined with polymeric material and form mixed matrix membranes (MMMs)[54] or synthesized on various supports for different purpose, such as polymer hollow fiber, tubular zeolite support and anodic aluminumoxide which expanded ZIFs application prospect.

2.2.3 ZIF-8

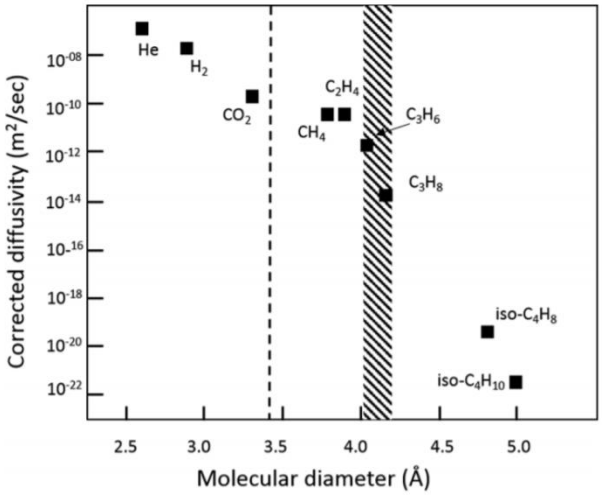

Figure 2.5 Diffusivities of various gas molecules versus their molecular diameters. Reproduced with permission.[55] Copyright 2015, Journal of Physical Chemistry C.

When it comes to propylene/propane separation, the desired aperture sizes of ZIF material need to fall between 4.0 to 4.3 Å as shown in figure 2.5. As the most well investigated member in ZIF family, ZIF-8 [11] has been thoroughly studied. Combined by coordination bond between zinc ions and 2-methylimidazoles, the crystallographically-defined aperture size of ZIF-8 is 3.4 Å,[11] it is marked in Figure 2.5 with a dashed black line. However, ZIF-8 has shown a clear through cut for gas mixtures between propylene (4.0 Å) and (4.2 Å) and hereby regarded as possessing an effective aperture size of 4.0-4.2.[15] Such a phenomenon bas cause by the flexibility between 2-methylimidazolate and Zn^{2+} ion. The linker of ZIF-8 are constantly in a flapping motion which is

commonly compared as "saloon door".[56] As a result, ZIF-8 provides perfect fitness for propylene/propane separation among ZIF family members.

Since the day it was first synthesized by park et al.,[11] ZIF-8 was then successfully synthesized into membrane [12] and showed impressive C2/C3 separation performance [13]. Intensive study on this ZIF member has never stopped. Pure well-intergrown ZIF-8 membrane was already synthesized by various method including hydrothermal seeded growth[13, 57-59], in situ growth[60-61], microwave-assisted seeding[12, 62-64] or electro-deposition [65-66] followed by secondary growth etc. The best defect-free ZIF-8 membrane was synthesized by Jeong et al. on alumina support with astonishing propylene/propane selectivity factor of ~200,[17] whereas the permeance of propylene, in another word, productivity, was only 157 x $10^{(-10)}$ mol $m^{(-2)}$ $s^{(-1)}$ Pa^{-1}. The robustness of ZIF-8 also leaves us adequate of potential for post-synthetic modification. Through a flexible coordination-based post-synthetic modification strategy, Wu et al. have made a poly (ethylenglycol) functionalized ZIF-8 composite membrane (ZIF-8/PEG-NH2) for water treatment.[67] 3-amino-1, 2, 4-triazole (Atz) functionalized ZIF-8 was proved effective for CO_2 absorption and related gas pair separation (CO_2/N_2 and CO_2/CH_4) due to confined gate sizes and pore volume by Cho et al.[68]

2.2.4 Ultra-thin ZIF membrane synthesis

Despite the promising future of ZIFs material and high performance compared to current commercial membranes, however, the current unit area cost for zeolite membranes is estimated to be €1,000 m^{-2},[69] and that of ZIF membranes is expected to be around $5,000 to $10,000 or higher

per square meter for an assembled module considering expensive organic ligands and solvents.[70] Just as Michael Tsapatsis pointed out,[71] high membrane manufacturing cost hinders the further development and implementations of MOF/ZIF membranes.[69] As such, the productivity or selectivity of current MOF/ZIF membranes must be significantly improved to overcome the prohibitively long payback times.

The membrane productivity can be defined by the following equation

$$Q_i = -\wp_i \cdot (\Delta p_i) \cdot A \cdot l^{-1}$$

Where $\wp_i$, Δp_i, l, and A are the permeability of gas i, partial pressure difference between feed and permeate sides of gas i, membrane thickness, and membrane area, respectively.[72] Either by increasing the membrane area or decreasing the membrane thickness, the productivity could be enhanced. By using polymer hollow fibers, tubular and carbon tubes supports, some of the ZIF membranes have been made with expanded surface area and shown selectivity but compared to planar support, the drop of selectivity and the complexity of synthesize procedure exceeded our expectation. So far, the attempts in enlarge membrane surface area have not achieve any substantial improvement in productivity.

On the other hand, reducing membrane thicknesses increases the membrane productivity seems to be more feasible. Various methods have been employed to reduce the thickness of polycrystalline membranes. Zhang et al.[73] reported an ultrathin ZIF-8 membrane (~ 550 nm) prepared by a spatially confined contra-diffusion process. He et al.[65, 74] demonstrated the syntheses of ultrathin highly intergrown ZIF-8 membranes (~ 500 nm) on various support using

electrophoretic deposition methods. Hou et al.[75] used a facile immersion technique to synthesize ultrathin ZIF-8 membrane (~ 400 nm). Hu et al.[76] prepared a defect-free ZIF-8/graphene oxide (GO) membrane (~ 100 nm) using two-dimensional (2D) ZIF-8/GO hybrid nanosheets as seeds. Li et al.[77] successfully synthesized nanometer-thick ZIF-8 membranes (~17 nm) through gel-vapor deposition. The paralyzed membrane on AAO support prepared by Caro et al. has shown both promising propylene-propane selectivity as well as permeance. [78] Nevertheless, current synthesis methods only produced very few membranes with impressive propylene/propane separation performance since the porous structure and surface roughness of most supports is tough to deal with, so the grain boundary structure of the membrane will be easily compromised after downsizing. The use of pricy chemicals/materials (e.g. polydopamine, (3-Aminopropyl) triethoxysilane, anodized-alumina supports (AAO)), or unconventional synthesis methods could mitigate the problem to some extent but it tends to defeat its original purpose of capital-saving. Hence a more universal, scalable synthesis method of well-intergrown ultrathin membrane with satisfying performance membrane is highly desired.

2.3 ZIF-67

2.3.1 Introduction

In general, ZIF-67 is Co-substituted ZIF-8. Due to the activity difference between Co and Zn, Co has considerably higher potential in Zn/Co−N bond and N−Zn/Co−N angle as shown in Figure 2.6,[18] which leads to stiffer bonding of Co with the adjacent N atoms results in a more rigid

structure with a smaller oscillation of the gate-opening therefore smaller aperture size.[19] The spectroscopic evidence provided by Kwon et al.[20] have also proved the restricted flapping motion of mIm linkers in ZIF-67. Therefore ZIF-67 possess narrower distribution of effective aperture sizes by both experiments [20, 32] and computations,[18-19] thereby potentially better propylene/propane selectivity than ZIF-8.

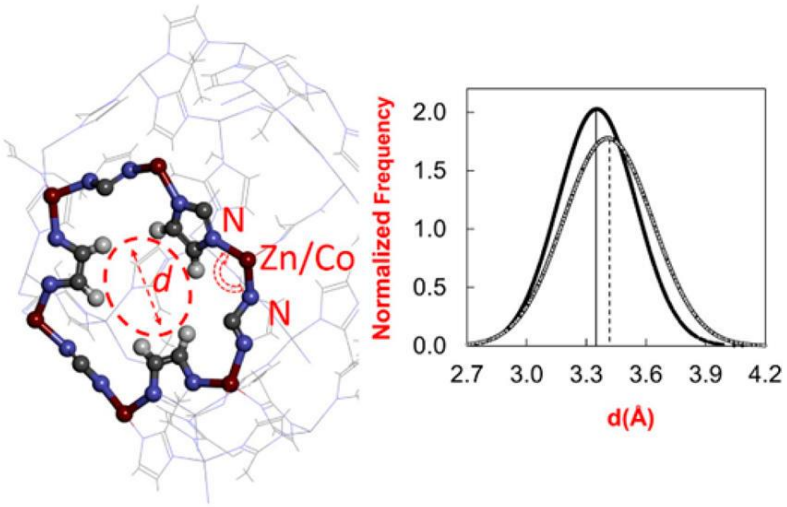

Figure 2.6 A Schematic illustration of structure difference between ZIF-67 and ZIF-8 (left) and their pore size distribution (right). The diameter on the x-axis indicates crystallographic pore size. Reproduced with permission.[18] Copyright 2016, Journal of Physical Chemistry C.

From the aperture size distribution in Figure 2.6, there is approximately 0.1 Å difference between the critical aperture sizes of the two frameworks and the effective aperture size still falls in the feasible zone of effectively separating propylene/propane. As a result, ZIF-67 is potentially very promising as membrane material for propylene/propane separations. Nevertheless, phase-

pure, ultrathin ZIF-67 synthesis has always been problematic so the performance of ZIF-67 has not yet proven by membrane separations.

2.3.2 Previous work review

Syntheses of phase-pure ZIF-67 membranes turn out not straightforward, especially on common alumina-based supports. Kwon et al.[20] has successfully grown the first nano-scale thin ZIF-67 membrane of only 700 nm over a ZIF-8 seeding layer on porous α-Al_2O_3 substrates, comparing to ZIF-8 membrane thickness of 1.2-2 μm made by the same method.[79] Their membranes showed remarkable propylene/propane separation factor of ~200 with the high propylene permeance of ~110 GPUs (1 GPU= 3.34×10^{-10} $mol \cdot m^{-2} \cdot s^{-1} \cdot Pa^{-1}$), proved that ZIF-67 could be a promising candidate for propylene/propane separation. However, these membranes had to be grown heteroepitaxially over ZIF-8 membrane (i.e., ZIF-67/ZIF-8 composite membranes). While the direct syntheses of ZIF-67 membranes on substrate led to disk-shape impurities, which was later identified as cobalt-alumina layered double hydroxides (LDH, hereafter).[80] With the requirements of multiple heteroepitxial layers, the process turned much complicated and cost-intensive, let along the membrane total thickness have risen to over 2 μm which greatly hindered the transport of gas through the membrane.

Other than the attempt made by Kwon et al.,[20] as summarized in Table 2.1, multiple methods have been exploited for synthesizing ZIF-67 membranes however direct syntheses of phase-pure ZIF-67 membranes turn out not straightforward. Wang et al.[21] synthesized phase-pure ZIF-67 membrane by introducing $Co(OH)_2$ precursor using electrodeposition, yet no

propylene/propane separation was reported. Jiang et al.[81] provided another option by synthesizing nanoporous ZIF-67 embedded polymers on Teflon plates via solution evaporation method. By using a APTES (3-aminopropyltriethoxysilane)-treated tubular α-Al_2O_3 support, Zhang et al.[82] coated the support with Co-NWAs, upon which phase-pure ZIF-67 membrane were synthesized afterwards. Furthermore, the performance of these membranes was improved by heteroepitaxially growing ZIF-67 membrane on top of ZnO nanorods on a tubular α-Al_2O_3 support.[83] Pan et al.[84] has successfully synthesized zinc/cobalt mixed-metal membranes which is capable of separating propylene/propane with selectivity of 50.5 when 90% of cobalt been substituted by zinc. However, to the best of our knowledge, no phase-pure ZIF-67 membrane with any propylene/propane selectivity have been reported, and because of the difficulties in controlling the growth, most membranes synthesized above are loosely packed with great thickness.

Table 2.1 Previous research about ZIF-67 related membrane

Year	PI	Support	Seeding Method	Membrane	Membrane Thickness	Performance (S.F.)	Reference
2018	Zhongyi Jiang	Teflon Plates	Solution Evaporation	PIM-1/ZIF-67	80±5 μm	CO_2/CH_4 (16.8), H_2/CH_4 (11.4)	81
2018	Xiongfu Zhang	APTES-treated tubular α-Al_2O_3	Co-NWAs coated support	ZIF-67@Co-NWAs	1.7 μm	H_2/N_2 (14.7), H_2/CH_4 (15.3)	82
2018	Xiongfu Zhang	Tubular α-Al_2O_3	ZnO-induced heteroepitaxial growth	ZIF-67@ZnO nanorods tubular membranes	3 μm	H_2/CH_4 (45.4)	83
2018	Jurgen Caro	APTES-treated α-Al_2O_3 plates	75 cycles of layer-by-layer growth	ZIF-8@ZIF-67	180 nm	H_2/CO_2 (6.5) H_2/CH_4 (5.5)	85
2017	Haihui Wang	Porous metal substrate	Electrodeposited nanosheets	ZIF-67 on $Co(OH)_2$ nanosheets modified support	13 μm	H_2/CO_2 (8.2), H_2/N_2(9.0) H_2/CH_4 (12.4)	21
2017	H-, K Jeong	Polymeric	Solution sonication	Mixed matrix membrane (6FDA-DAM)/ZIF-67	10±1 μm	C_3H_6/ C_3H_8 (19, 21.1% loaded)	6
2017	Shaojun Dong	——	——	2D ultrathin ZIF-67 nanosheets	4.5 nm	——	86
2016	Yichang Pan	α-Al_2O_3 disk	Direct mixing of precursor solutions	Mixed metal (Zn and Co)	3.7 μm - 2.2μm	C_3H_6/C_3H_8 (1.4 for ZIF-67, with 50.5,90% Zn substituted)	84
2015	H-, K Jeong	α-Al_2O_3 disk	Microwave seeding	Heteroepitaxial growth of ZIF-67 upon ZIF-8	1.0 μm/1.5 μm	C_3H_6/C_3H_8 (209.1±8.5 ZIF-8/ZIF-67 163.2±30.9 ZIF-67/ZIF-67)	20

2.4 Fabrication Method

2.4.1 Direct Synthesis

The direct synthesis method typically immerses the support without any surface modification in ZIF synthesis solution where ZIF membrane could grow directly on substrate surface. Juro et al.[12] have synthesized promising ZIF-8 membrane through microwave-assisted solvothermal synthesis method on asymmetric titania support with membrane thickness around 25 μm while no gas pair selectivity was reported. Jeong et al.[60] optimized the growth by using an *in situ* method based on a counter-diffusion concept. Compared to previous results, the resulting membrane was well-intergrown with impressive propylene/propane selectivity over 50 and the thickness was only 1.5μm. Continuous MOF-5 membrane[87] and ZIF-69 membranes[52] could also be synthesized on solid support following the same approach.

Despite several achievements in ZIF synthesize, direct synthesize method have also encountered various bottlenecks. Given that the crystallization depends on various elements, only limited membranes with gas separation performance and acceptable permeance has been made. Forming a dense polycrystalline ZIF layer as required is extremely challenging through direct synthesis given that the interfacial bonding between the membrane and chemically inert support is weak, therefore membrane cracking and detaching problem is very common. Moreover, the crystallization process is lack of control so the resulting consequence is undesired nucleation in the solution or growth on top of previously formed crystals instead of the growth on the support.[88] In many cases, this problem would lead to extra amount of synthesize solution usage thereby increase the cost and cause incomplete support coverage. Due to the porous material support we currently use, direct synthesis will also lead to unevenly distributed crystal sizes which would further develop into uneven membrane thickness with defects and oversize inter-crystal voids.

Although some effective defect healing technologies have been proposed to deal with the compromised structure issue,[60] the complexity of the procedure and resulting high membrane thickness still hindered it from massive application.

As a result, to fabricate integrated membranes, we need a new approach with better crystallization and the following growth control. In addition, the membrane needs to be firmly anchored with the support.

2.4.2 Seeded Growth

Membrane synthesis methods can be assorted into two categories, direct synthesis methods and seeded methods. Seeding procedure followed by a secondary growth has been proved feasible in producing well-intergrown, defect-free ZIF membranes. Benefiting from the decoupling of nucleation and growth, seeded growth generally offers better control of the microstructure of the membrane and stronger anchored on porous supports over the direct synthesis method.

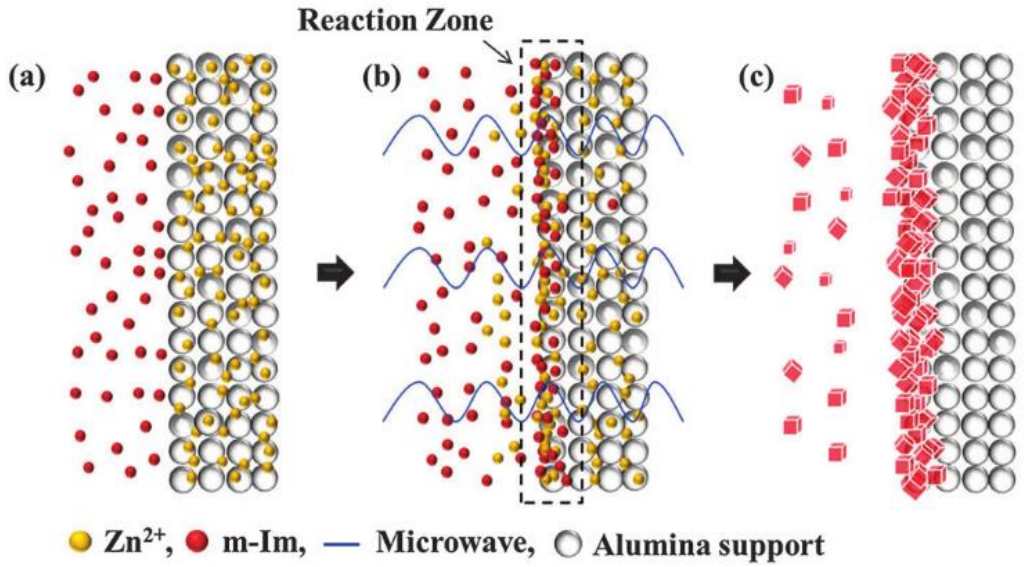

Figure 2.7 A Schematic illustration of a typical rapid microwave-assisted seeding process for ZIF-8. Reproduced with permission.[79] Copyright 2013, Chemical Communications.

Among all seeding methods (polymer binder-assisted, thermal, *in situ* seeding), traditional microwave seeding method[12, 72, 79, 89-90] can provide seeding crystals not only strongly attached but also densely and evenly distributed as shown in Figure 2.7. This seeding process has proved its value in multiple membranes synthesis[79, 87, 91-92] and resulting membranes usually show well-formed structure and better gas separation performances. The formation of densely-packed seeding nanoparticles also provides an unprecedented opportunity for ultra-thin, phase-pure ZIF-67 synthesis. However seeds with smaller size were needed for thinner ZIF-67 membrane since the traditional microwave seeding process would form much bigger seeds and thereby membranes with greater thickness. And introducing amines (e.g. triethylamine, hereafter TEA)[33, 93-94] into the system can greatly reduce the size of ZIF crystals by promoting the deprotonating process of organic linkers. With the help of TEA, sub-micron ZIF-90,[95] nanosized ZIF-67 particles,[96] have been successfully synthesized. TEA has also been proved effective in controlling facet growth and crystal morphology in the microwave seeding step.[95-98] More details can be found in chapter Ⅳ.

Since the size of support particle is much larger than our target ZIF-67 seed size, the surface roughness problem still exist given that the voids between seeded support particle remain unfilled. Kumar et al.[74] have proposed a novel ENACT seeding method (electrophoretic nuclei assembly for crystallization of highly intergrown thin-films) by using which a layer of crystals with controllable size can be deposited on the surface of support caused by the surface charges. As such, not only the surface of the support would be smoothed by crystals induced by ENACT, each crystal will also be able to growth a short extend and therefore reduce the thickness of the membrane. By combining the above two seeding approaches, we can obtain better control over ZIF synthesis and growth.

2.4.3 Post-synthetic linker exchange (PSLE)

Restricted by synthesis condition, the function and diverse range of ZIFs is still somewhat limited, it is possible to modify the ZIFs structure by postsynthetic modifications which means controlling over both the type of substituent and the degree of modification directly on synthesized membranes. The versatility of a well-formed ZIF membrane could be enhanced by introducing multiple functional groups into it in a combinatorial manner, enabling an effective way to systematically fine-tune and optimize ZIF properties.[99] Multiple attempts have been made in related area. Han et al.[100] showed that the microcavity size of microporous material could be tuned by thermal rearrangement and Wang et al.[99] discussed the wide application of post-synthetic modification technique in detail. Relative studies in post-synthetic modification have been reported, such as introducing redox-active transition metal,[101] solvent-assisted linker exchange[102] and others.[72, 101, 103-104]

Recently, Jeong et al.[72] reported the modified ZIF-8 membranes (ICA-ZIF-8) by introducing the ICA (2-imidazolecarboxaldehyde, linker for ZIF-90) ligands into the ZIF-8 structure using a PSLE method as shown in Figure 2.8. Since ICA is bulkier and has less flapping motion comparing to 2-mIm, therefore less flexibility and the effective aperture size, the permeance of propylene was drastically increased while the SOD topology was not affected.[72] Considering the similar property of Zn and Co, the similar PSLE process is expected to be feasible. Therefore, for further improving the propylene permeance, the effective thickness of ZIF-67 membrane can be reduced by PSLE.

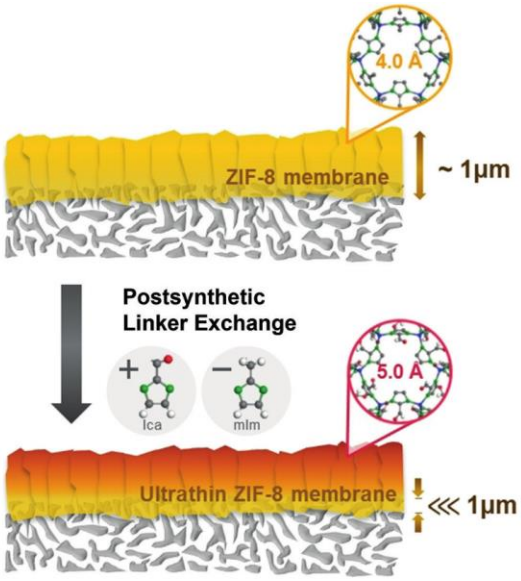

Figure 2.8 A Schematic illustration of reducing the effective membrane thickness by PSLE of mIm of ZIF-8 with ICA, the aperture size is enlarged. Reproduced with permission.[72] Copyright 2018, Angewandte Chemie-International Edition.

2.5 Challenges

2.5.1 Seed size control

As mentioned in the previous section, the formation of densely-packed seeding nanoparticles provides an ideal condition for phase-pure ZIF-67 synthesis. Since the crystals could be seeded deeply into the porous support, secondary growth on preexisting seeds generally provides better control over the microstructure of the membrane and stronger anchoring on porous supports. Although traditional microwave seeding method can provide strongly attached and densely packed seed layer, it results in seeds of 70-120 nm in size, therefore membranes as thick as 1.5 μm,[79] and consider the porous structure of α-Al_2O_3 we used, there is also still voids between seeds that remain unfilled due to support surface roughness, which will eventually lead to formation of impurities or compromised grain boundary. Therefore, the seeding method needs to be modified for ZIF-67 membrane synthesis.

The first step is to downsize the crystal seeds. According to previous research,[96] by introducing TEA into the system as deprotonator, the nucleation rate will be significantly improved and the size of the seeds will be decreased below 50 nm. When excessive amount of TEA is applied, the nucleation process would actually be impeded and the resulting product appears to be amorphous state so it wouldn't show any obvious crystal structure pattern after XRD tests. The detailed result will be discussed in chapter Ⅳ.

The second crucial step is to fill out the gaps and hollow pores with bigger size seeds. As mentioned in the last section, ENACT has provided a novel way to deposit another layer of seeds upon microwave-seeded support. However, the concentration of metal and ligand solution, aging time and reaction time need to be strictly controlled to guarantee the proper amount of seeds with correct size are seeded. If the support is over-seeded, the resulting membrane will be thick and poorly attached, the anchoring effect of microwave seed base layer will also be diminished. If inadequately seeded, the impurities will appear after secondary growth. In sum, the seeding step is actually the most vital step in the whole synthesis process, it requires precise control over the amount and size of the seeds as well.

2.5.2 Temperature control

The temperature control of secondary or even tertiary growth is another crucial parameter considering the early stage of nucleation is extremely temperature sensitive. Since we are using an autoclave-lined reactor, the wall of the container will be the first to be heated, regarding the Ostwald-ripening effect,[105] the nucleation tend to start around the wall and form crystal particles. The seed layer synthesized in the seeding step, on the contrary, will be dissolved into the solution and join the crystallization process around the wall which will expose the α-Al_2O_3 support that was originally fully covered and lead to LDH formation.

Programmed heating is needed for secondary and the following growth. However, if the temperature is too low to cross the activation energy barrier, the process would be hindered so an optimized temperature has to be found in the experiment. During the following PSLE process, since the ICA is more active than mIm, an improper linker exchange temperature might lead to the collapse of crystal structure and compromise the perm-selectivity. An over-intensive exchange process will also result in membrane defects.

2.5.3 The formation of impurities

When Kwon et al.[20] tried to synthesis ZIF-67 membrane directly on α-Al_2O_3 support, an unknown disk-shape impurity was observed. In the following experiment process, the similar kind of impurities was observed again as shown in Figure 2.9. None of those impurities was found after microwave seeding step or ENACT seeding step which means secondary growth is crucial for impurity forming.

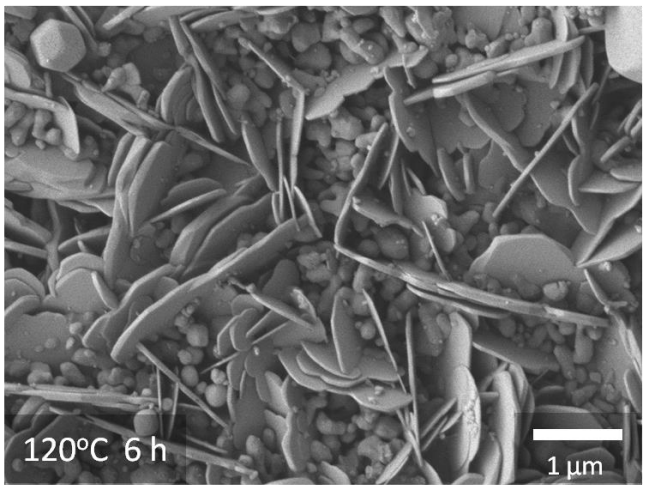

Figure 2.9 The SEM image of disk-shape impurity we observed on the α-Al_2O_3 support (top view). The temperature and time marked on the bottom left corner indicates the secondary growth condition we used.

Later on, the impurity has been characterized as cobalt-alumina layered double hydroxides by Kamath et al.[80] Typically obtained by partial isomorphous substitution of M(II) ions by M'(III) ions in the structure of $M(II)(OH)_2$, LDHs can further capture CO_2 in the atmosphere and crystallize with carbonate ions in the interlayer region. The resulting product could be expressed as $[Co\text{-}Al\text{-}CO_3]_{0.33}$ which is extremely stable so it can only be dissolved by using mineral acid once it's formed. Therefore, the vital issue in this case is to control the exposure of support to minimize the Al^{3+} in the solution.

Concerning the membrane cracking problem induced by uneven expansion due to rapid cooling, the membranes we synthesized were cooled down naturally at room temperature. It turned out that the CO_2 in the air is adequate to be captured and turned into LDHs, so the membranes should only be rapidly dried in convection oven. The formation of LDHs is also the reason why we need this novel combined-seeding method to fully cover the substrate surface and prevent seed dissolving problem in the following growth steps by controlling the temperature and growth time.

CHAPTER III

EXPERIMENTAL SECTION

3.1 Chemicals

To prepare disk-shaped alumina substrate, α-Al_2O_3 powder (CR6, Baikowski) was pressed with polyvinyl alcohol (PVA 500, Duksan) solution as the binder. To synthesize ZIF-67 membrane, Cobalt nitrate hexahydrate ($Co(NO_3)_2$ •$6H_2O$, 98%, Sigma-Aldrich) was used as metal source while 2-methylimidazole (2-mIm, hereafter) ($C_4H_6N_2$, 99%, Sigma-Aldrich) as organic ligand source. Triethylamine ($C_6H_{15}N$, 99%, Fisher Chemical, hereafter TEA) was applied as deprotonating agent in microwave seeding step. The deionized water or methanol (CH_3OH, >99%, Alfa Aesar) were used as solvents. 2-imidazolecarboxaldehyde ($C_4H_4N_2O$, 97%, Alfa Aesar, hereafter ICA) was used for ligand exchange experiments. All chemicals were used as received without any further purification.

3.2 Experiments

3.2.1 Preparation of α-Al2O3 substrate

Disk-shaped alumina substrates (porosity = ~ 46 %, diameter = 22 mm, and thickness = 2 mm) with an average pore size of ~ 200 nm were prepared by the previously reported method.[20] In summary, 10 g of α-Al_2O_3 power was mixed with 1 ml of PVA binder solution followed by continuous grinding until aggregated powder was completely shattered. After that, 2.1 g of the grounded powder was molded into a disk-shape mold by exerting 17 MPa of pressure for 1 min and sintered at 1100 ^oC for 2 h afterwards. The sintered disks were polished on one side using a sand paper (grid #1200) to reduce the surface roughness of the substrates and to remove the particle

residue, following by sonication for 1 min in methanol to further remove debris from polishing step. Subsequently the supports were dried in an oven at 120 ^{o}C for 1 h before usage.

3.2.2 Preparation of ZIF-67 seed layers using microwave-assisted seeding

For microwave seeding, precursor solutions were prepared following the previously reported method.[96] Briefly, a metal solution was prepared by dissolving 472 mg of cobalt nitrate hexahydrate into 40 ml of methanol and a ligand solution prepared by dissolving 532 mg of 2-mIm in 40 ml methanol as well as 48 µl of TEA. The α-Al_2O_3 substrate made previously was immersed in metal solution and held vertically using a self-made Teflon holder. After 1 h of soaking, the saturated substrate was quickly moved into ligand solution in a microwave-transparent tube and tube was immediately inserted into microwave oven for 1.5 min with 100 W power capacity, followed by 30 min cooling down in room temperature. The support was then washed in 40 ml methanol under gentle rocking for 12 h then dried in a convection oven at 60 ^{o}C for another 4 h before further experiments.

3.2.3 ENACT seeding process upon microwave-seeded substrate

The ENACT seeding was conducted following the previously reported method with a few modifications.[74] Briefly, the microwave-seeded α-Al_2O_3 substrate from the last step was fully dried then attached to a copper electrode (cathode) while the other copper electrode was used as anode. Be aware, the copper electrodes need to be carefully polished using sand paper (grid #400) to remove the oxidized layer before usage. Both electrodes were connected to an external power source (HYELEC HY3005B) which can provide stable direct current. A metal solution was prepared by dissolving 0.44 g of cobalt nitrate hexahydrate in a mixture of 2.5 ml of methanol and 17.5 ml of D.I. water while a ligand solution was prepared by dissolving 11.08 g of 2-mIm in 2.5 ml of methanol and 17.5 ml of D.I. water. The metal solution was first poured into the ligand

solution followed by mixing for 30 s under stirring. Next, the electrodes and the seeded substrate were soaked into the mixed solution followed by a 3-min aging process. A constant voltage of 1 V was then applied between the electrodes for 4 min with the distance between the electrodes equal to 1 cm. After the ENACT process, the support was carefully rinsed then immersed in 40 ml of methanol for 12 h to wash off unwanted residues and then dried in a convection oven at 60 ^{o}C for 4 h before the secondary growth.

3.2.4 Secondary growth (SG, hereafter)

Ligand and metal solutions were prepared by dissolving 2.27 g of 2-mIm and 0.11 g of cobalt nitrate hexahydrate in a mixture of 2.5 ml of methanol and 17.5 ml of D.I. water, respectively. These solutions were then mixed for 2 min in a Teflon-lined autoclave with the seeded alumna substrate inside. The seeded substrate was held vertically using a self-made Teflon holder. The reaction was carried out in a convection oven with a temperature program. The autoclave was first preheated to 40 ^{o}C for 10 min and then the oven was gradually heated up to 70 ^{o}C in 1.5 h and maintained constant for 24 h. After the secondary growth, the autoclave was cooled down to room temperature. The resulting membrane (hereafter, SG-ZIF-67 membrane) was washed in 40 ml of methanol for 1 day and dried in a convection oven at 60 ^{o}C for 4 h before further characterizations and permeation tests.

3.2.5 Tertiary Growth (TG, hereafter)

A secondarily-grown ZIF-67 membrane was first washed and dried then treated with a ligand solution (solution of 4.54 g of 2-mIm in a mixture of 5 ml of methanol and 35 ml of D.I. water) in a Teflon-lined autoclave we used for SG at 120 ^{o}C for 4 h. No programmed heating was needed. Then the ligand-treated membrane was cooled down naturally to room temperature and then washed in 40 ml of methanol overnight and dried in 60 ^{o}C for 4 h. Tertiary growth followed

the same procedure as secondary growth. The as-prepared tertiarily grown ZIF-67 membrane (hereafter TG-ZIF-67 membrane) was washed and dried same way as mentioned above for future characterization and test.

3.2.6 Post-synthetic linker exchange (PSLE)

0.1 g of ICA was dissolved in 40 ml of methanol under heating and stirring. The heating temperature for ICA solution was maintained at 55 ^{o}C to prevent the boiling of methanol. Ligand exchange procedure was adopted from the previously reported one by Lee et al.[72] In short, a SG-ZIF-67 or TG-ZIF-67 membrane was treated solvothermally in an autoclave with the ICA solution at 60 ^{o}C for different time period from couple of hours to 2 days. To maintain a uniform temperature, all containers were preheated to 60 ^{o}C before experiment. The ICA-exchanged membrane was then cooled down to room temperature and washed for 24 h in 40 ml of methanol and dried for 4 h at 60 ^{o}C.

3.3 Characterizations

The permeation test was carried out on a home-built Wicke-Kallenbach setup with an argon flow of 100 ml/min as sweep gas on the permeate side and 100 ml/min 50:50 propylene/propane gas mixture on the feed side (see Fig 3.1 for more details). The permeate side composition was characterized using an Agilent GC 7890A gas chromatography (equipped with HP-PLOT/Q column).

Scanning electron micrographs of both membrane surface and cross section were collected with a JEOL JSM-7500F system operated with an acceleration voltage of 2 keV with a working distance of 15 mm. Since the conductivity of ZIF-67 was not ideal, all samples were coated by platinum with thickness of 5 nm prior to SEM. After PSLE experiment, the membrane became

more sensitive to the electron beam so some cracking problem would appear in some of the surface SEM pictures. Powder X-ray diffraction (PXRD) patterns were collected using a Rigaku Miniflex II powder diffractometer with Cu-Kα radiation (λ = 1.5406 Å). The pattern of our sample was compared to computer simulation result to confirm the crystalline structure or if there was any impurity phase formed.

A NICOLET IR100 FT-IR spectrometer was used for characterization of linker exchange. However, this is just a rough estimation, more detailed solution ^{1}H NMR spectra were obtained by an INOVA300 spectrometer at RT. ^{1}H NMR samples were prepared using a CD_3OD solution including 0.02 vol% of H_2SO_4.[68]

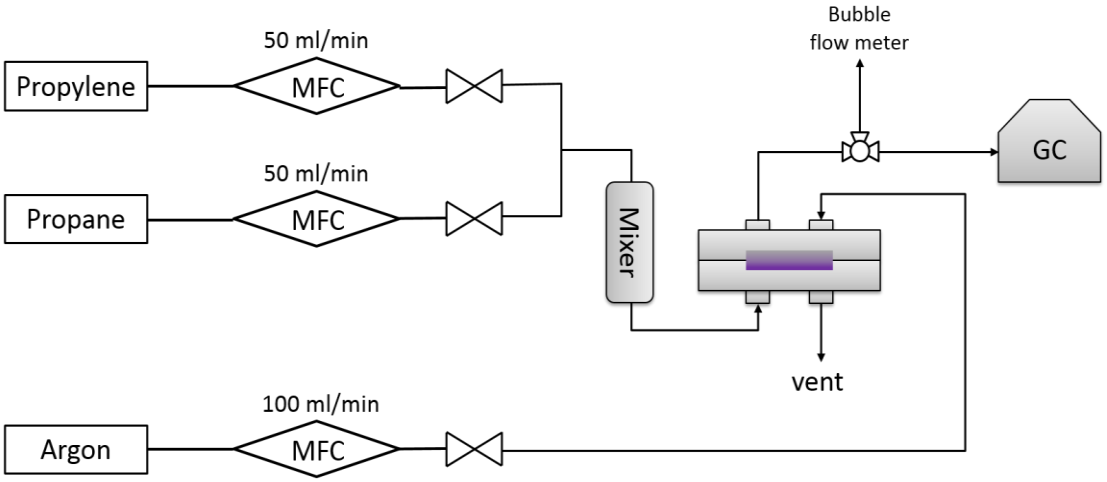

Figure 3.1 Schematic diagram of a gas permeation set-up (Wicke-Kallenbach technique).

CHAPTER IV

RESULT AND DISCUSSION

Forming only two coordination bonds with nearby zinc ions, the linkers of ZIF-8 are geometrically flexible and constantly in a thermal-driven flapping motion which is commonly analogized as "saloon doors".[56] Ascribe to the flexibility of its framework, ZIF-8 has shown its value in effective propylene/propane separation. As discussed in chapter III, comparing to Zn-N coordination bonds in ZIF-8, Co-N bonds are mechanically stronger, therefore ZIF-67 has been predicted to possess more rigid structure thereby smaller effective aperture sizes and higher selectivity when made into membranes.[19] The intrinsic C_3H_6/C_3H_8 selectivity of ZIF-67 was estimated to more than 4 times higher than that of ZIF-8.[18] Therefore, ZIF-67 is inherently a promising membrane material for propylene/propane separation.

ZIF-8 membranes prepared by microwave-assisted seeding and secondary growth methods,[79] have been proven of high quality because of the densely-packed seed layers strongly attached on alumina substrates after the seeding.[17, 20, 53, 106] However, applying the same methods to ZIF-67 can be problematic, according to Kwon et al.[20] During the microwave-assisted syntheses of ZIF-67 membrane on substrate, the cobalt ions in the solution combining with the alumina leached from the support formed disk-shape impurities, which was confirmed as $[Co\text{-}Al\text{-}CO_3]_{0.33}$ LDH.[80] To avoid such a leaching process, a denser coverage of ZIF-67 crystals on the support should be provided to avoid the contact between the secondary growth solution and the alumina support for suppressing the formation of LDH impurities.

4.1 Seeding steps

Figure 4.1 illustrates the overall process to obtain high-quality seed layers by microwave seeding combined with the ENACT process. With the presence of TEA, nanosized seeds are firstly deposited by rapid microwave-assisted seeding process on the surface of α-Al_2O_3 support to provide good anchoring effect. Bigger seeds aiming at filling the voids between the support particles are seeded afterwards by ENACT process. To prevent subsequent membrane from growing over-thick, the extra seeds deposited in ENACT will be washed off thoroughly followed by multiple growth procedures, eventually leading to well-intergrown, ultra-thin ZIF-67 membranes.

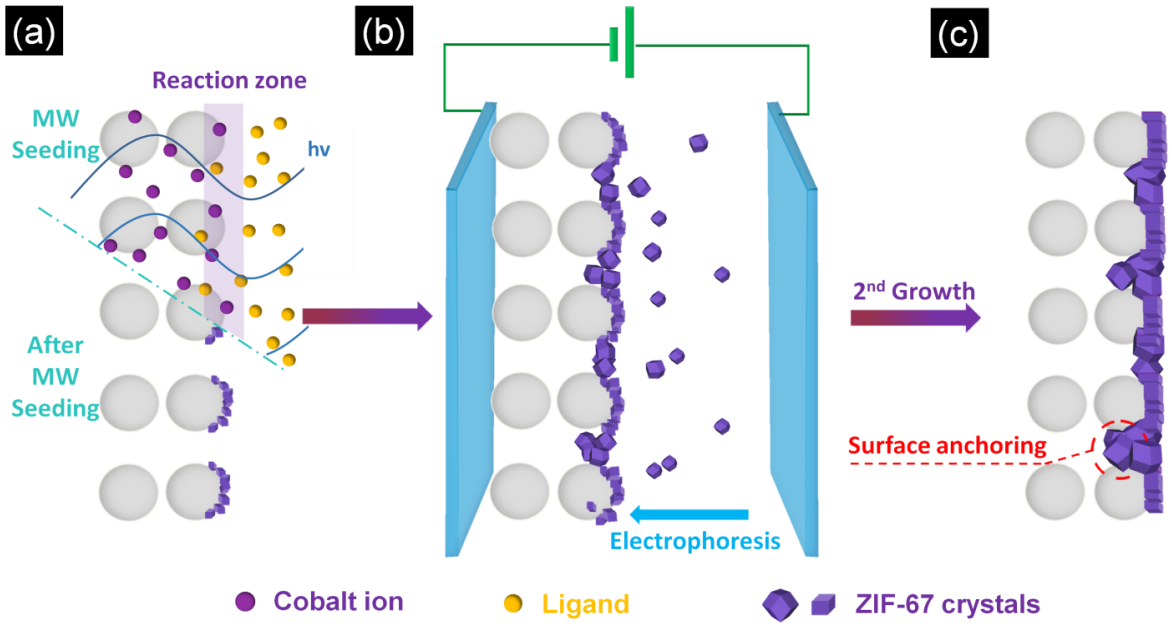

Figure 4.1 Schematic illustration of combined seeding process: (a) the microwave-assisted seeding step, (b) the ENACT seeding step, and (c) the secondary growth.

4.1.1 Microwave seeding optimization

As shown in Figure 4.1a, to enhance ZIF-67 nucleation rate, TEA was used during microwave seeding, forming seed layers of ZIF-67 nanocrystals. Traditional microwave-seeding approach without any amine additives, as a matter of fact, will only lead to few, extremely big particles. As shown in Figure 4.2, after MW treatment under 100 w and 90 s, crystals over 500 nm of size are deposited which are obviously oversized compare to the surrounding support particles. The support after MW treatment could barely observe any purple color on top which means inadequate of crystals were formed, indicating extra amine additive is necessary for crystallization process.

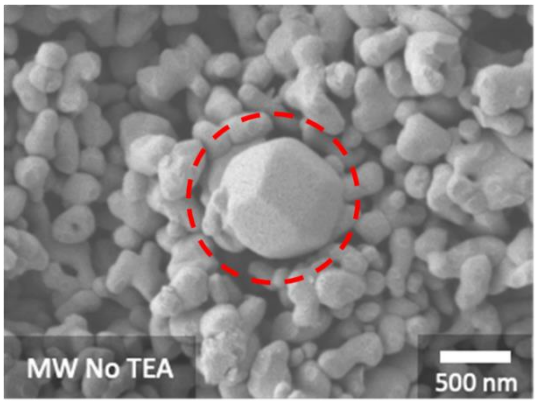

Figure 4.2 SEM image of microwave seeded support without TEA

The Introduction of amines including TEA [33, 93-94] into the reaction system have been proven greatly reducing the size of ZIF crystals by promoting the deprotonation of organic linkers. Zhang et al.[96] has studied the effect of TEA on ZIF-67 crystal size in detail and they found that the particle size decreased from 900 nm to 20 nm when increased the use of TEA from 2 μL to 12 μL. Liguori et al.[95] also reported sub-micron ZIF-90 in methanol solution with the presence of TEA. TEA has also been proved effective in controlling the forming of facets as well as crystal

morphologies.[95-98] Wang et al.[97] controlled facet growth of MOF-5 and tuned its size and shape during its crystallization with TEA as additional base. Yang et al.[98] investigated the effect of TEA on morphology and size of SUMOF-3 microcrystals. By introducing TEA into the system, the mIm in Figure 4.3 was first deprotonated by amine therefore more reactive sites on the ligands to facilitate the reaction with metal ions. Consequently, the nucleation is initiated and accelerated so the formation of small particle was prompted. However, mentioned by Matsuura et al., [93] if exceeded amount of TEA was added, the high reaction rate might lead to the formation of some impure component which might lower the mass yield.

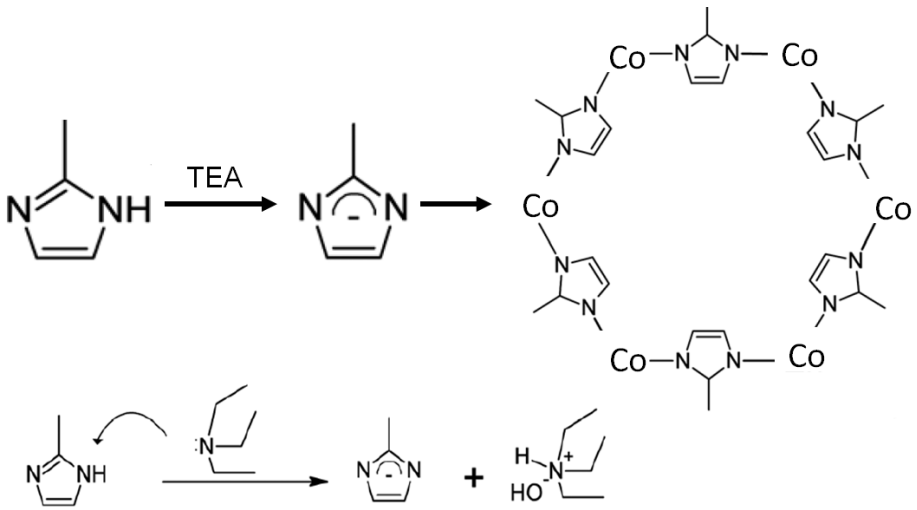

Figure 4.3 Schematic illustration of TEA in deprotonation process of mIm. Reproduced with permission.[93] Copyright 2014, Rsc Advances.

As shown in Figure 4.3a, the size of seeding crystals was significantly reduced from ~600 nm (see Figure 4.2) to ~20 nm in the presence of TEA and the density of seed crystals was drastically increased upon optimization of microwave conditions. However, when TEA amount exceeded 48 μL, there would be no peak on XRD pattern, showing facet forming has been impeded. Also the purple color of seeded support turned much lighter than previous TEA

concentration. It is possible that when extra TEA is applied, excessive dissociated water will also coordinate with ligands and form hydroxylated mIm which will result in crystal irregularities. As can be seen in Figure 4.4, the seed crystals were grown on the surface of the alumina grains, leaving large voids between the grains, which is not suitable for the synthesis of ultrathin membranes. Seeds of 50 nm or bigger will be needed to fill out those gaps.

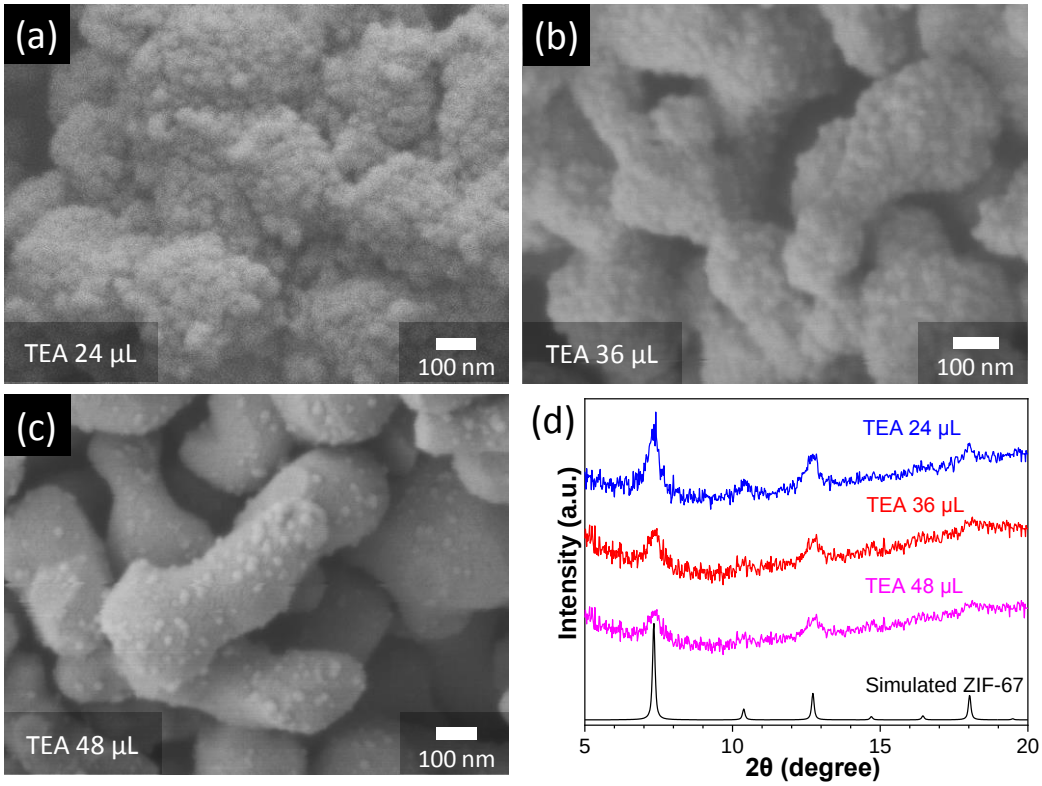

Figure 4.4 Optimization of TEA content during microwave seeding. Top-view SEM images of microwave seeded support with different TEA content (a-c) and their corresponding XRD patterns (d).

4.1.2 ENACT seeding

As shown in Figure 4.1b, to fill the voids between the alumina grains, an ENACT process was applied.[65, 74] The electrophoretic nuclei assembly for crystallization of highly intergrown thin-

films process was reported by Dr. Kumar's group and can provide a precise control over the crystal sizes during surface depositions on various supports simply by varying the aging time and the deposition time. The coulombic interaction between the surface charges (characterized by the zeta potential) and the external electrical field enables deposition of newly formed crystal nuclei. Important parameters of this process include the aging time after mixing the ligand and metal solutions, voltage applied between the electrodes, and deposition time so that proper amount of seeds with desired size might be deposited.

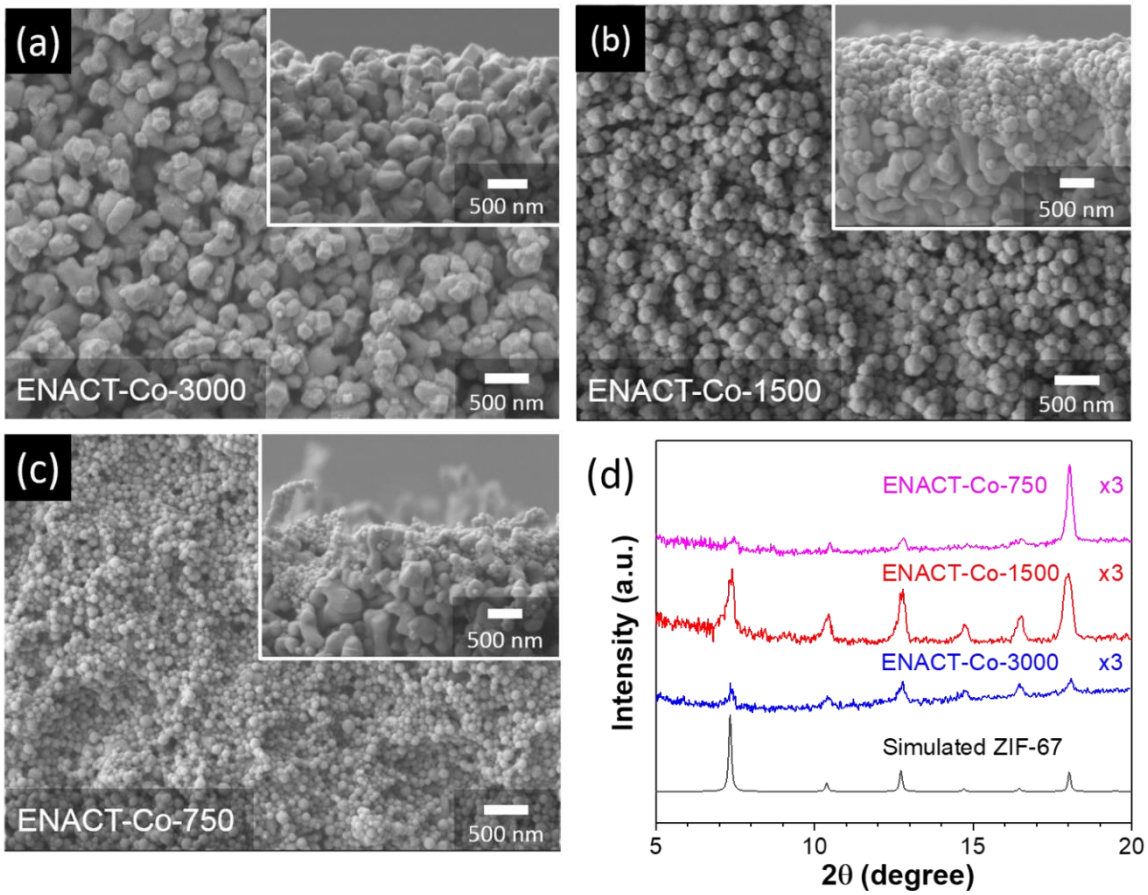

Figure 4.5 Optimization of ENACT content during microwave seeding. Top-view SEM images of microwave seeded support with different metal and ligand concentration (a-c) and their corresponding XRD patterns. ENACT-Co-3000/1500/750 stand for a metal to ligand to methanol ratio of 1:72:3000/1500/750 with 48 µl Triethylamine (TEA).

To control the seed size in ENACT step, we have tested four different solvent/metal/ligand ratio with TEA (Figure 4.5) which was proved to be effective in seed downsizing. However, it should be noticed that there is a upper and lower bound for amount of TEA been used, poor crystallinity or crystal facet forming caused by TEA insufficient or overdose is found in both ENACT-Co-750/3000 groups. Seeds in Figure 4.5b seem to have the best crystallinity yet they were oversized. The solution to this problem is by prolonging the aging time without TEA so the deposition process was not initiated until there was already quite amount of particles formed in the synthesis solution. After optimization, seeds size have been reduced to 50~70 nm which is just right for gaps between seeded support particles.

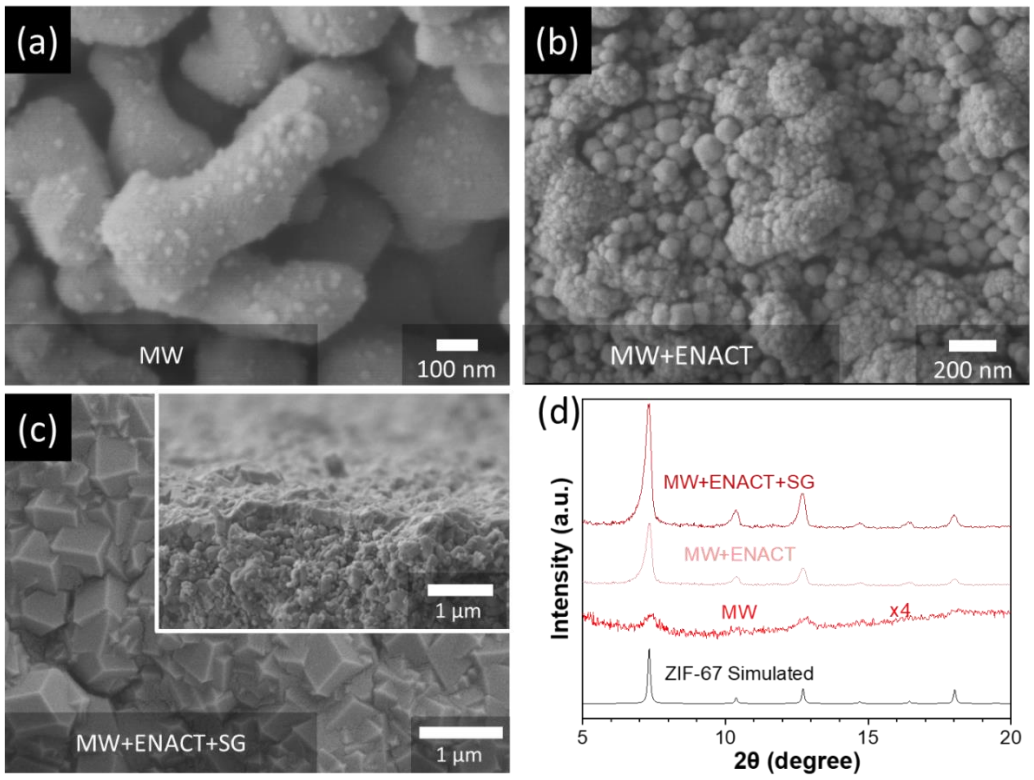

Figure 4.6 SEM images of (a) support after microwave seeding with TEA (48 µL), (b) support after combined seeding process, (c) continues membrane after combined seeding then secondary growth and (d) their corresponding XRD patterns. MW, ENACT, SG stand for microwave seeding, ENACT seeding and secondary growth, respectively.

Upon optimization of the above-mentioned parameters (see Figure 4.6), the ENACT seeding enabled the deposition of ZIF-67 nanocrystals (~ 70 nm) onto microwave-assisted seeded supports. As can be seen in Fig 4.6b, there was a bimodal distribution of crystals after ENACT seeding. It is likely that these smaller crystals with a size of ~30 nm on alumina grains were microwave-seeded crystals after grown during the ENACT process. The larger crystals found in the inter-grain spaces were deposited onto the support because of the static electrical field induced externally. Consequently, the seeded support showed densely-packed seed layers with a bimodal distribution (~ 30 nm and ~ 70 nm) of ZIF-67 nanocrystals. As such, not only the surface of the support would be smoothened by ENACT crystals, each crystal will also be able to grow a shorter extend, therefore reducing the thickness of the membrane. The resulting phase-pure ZIF-67 membrane showed well-formed structure with thickness less than 500 nm as shown in Figure 4.6c and no impure components been observed in its corresponding XRD pattern (Figure 4.6d). The following growth method will be discussed in the next section.

4.2 Secondary and tertiary Growth

4.2.1 Secondary Growth

As mentioned in chapter Ⅱ, to prevent the formation of LDH impurities, we need full coverage of α-Al_2O_3 support particles to eliminate direct contact between Al^{3+} and solution. By following the same growth condition under 120 ^oC described by Kwon et al.,[20] the Ostwald-ripening phenomenon caused seeds dissolution by heating the autoclaves directly then lead to the formation of LDH impurities. Therefore, we set up a programmed heating process as shown in

Figure 4.7a, pre-heat the reactor at 40 °C followed by continuous warming for 1.5 hr until set point temperature.

Since the seeding process involves multiple steps, it turned out a bit challenging to consistently obtain quality seed layers. If there's LDH formed, the corresponding peak should locate between (002) and (112) peak of ZIF-67. From the XRD result in Figure 4.7c, there is only a LDH peak after secondary growth while the MW and ENACT process seems to be normal which indicates the massive exposure of support particles still exists. Meanwhile, from the result listed in Table 4.1, there was no separation performance toward propylene/propane after growth at 120 °C. The structure of $[Co\text{-}Al\text{-}CO_3]_{0.33}$ can be inferred from $[Zn\text{-}Al\text{-}CO_3]_{0.33}$ shown in Figure 4.7b considering their similarities in both crystal structure and metal chemical properties. To minimize the CO_2 in the system which is crucial to prevent LDH formation, all drying process was conducted in convection oven under 60 °C. It was hypothesized that the LDH formation reaction can be hindered by lowering the temperature from 120 °C at which the secondary growth was performed.

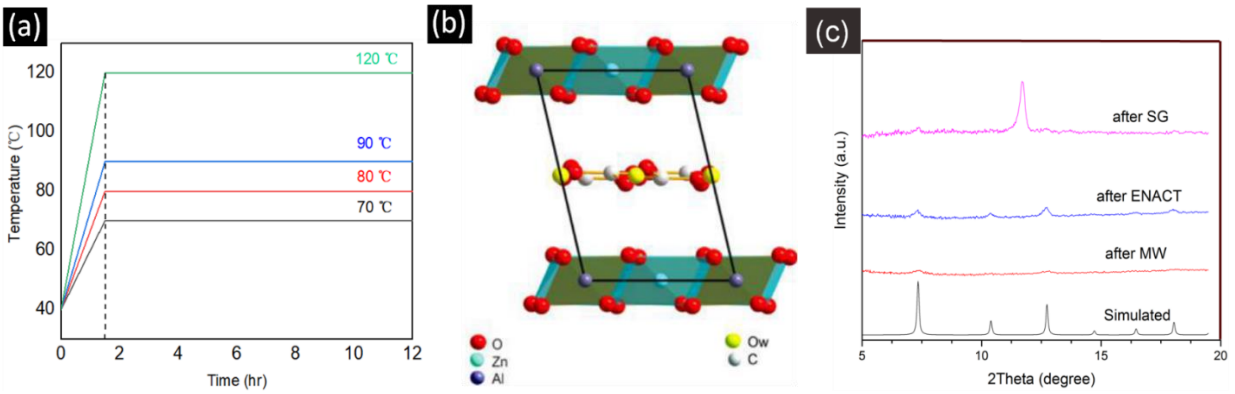

Figure 4.7 Illustration of programmed heating process (a) and complete unit cell of $[Zn\text{-}Al\text{-}CO_3]_{0.33}$ showing the carbonate ions in the interlayer (b) and the whole synthesis process XRD pattern (secondary growth under 120 °C) (c). Reproduced with permission.[80] Copyright 2015, Industrial & Engineering Chemistry Research.

After decreasing the SG temperature to 80 ^{o}C and 90 ^{o}C, the LDH peak still exist (see Figure 4.8d) however the intensity significantly decreased. No disk-shape structure was observed from the surface SEM pictures but deep inside, at the layer between the membrane and support, few LDH disks could be found. Fortunately, the performances start to show some improvements. When the secondary growth temperature decreased to 70^{o}C, the diffraction peak of the impurity completely disappeared, a phase-pure ZIF-67 membrane less than 500 nm thick was made.

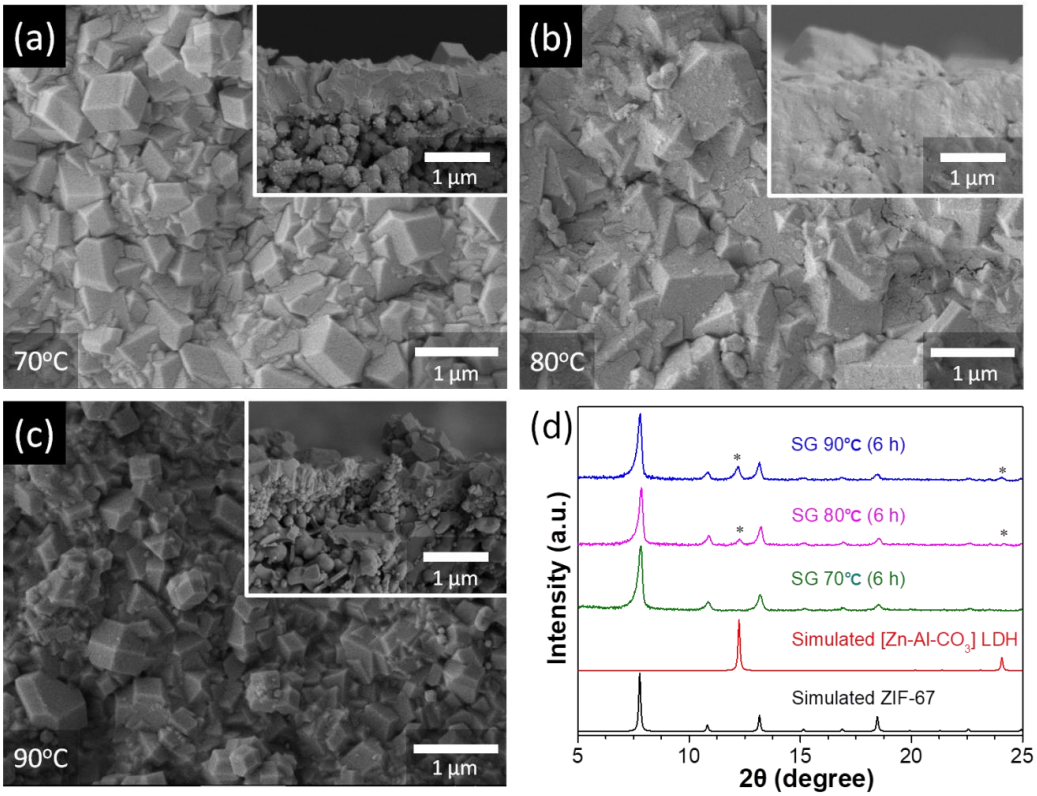

Figure 4.8 SEM images of ZIF-67 membranes at (a) 90^{o}C, (b) 80^{o}C and (c) 70^{o}C and their corresponding XRD patterns (d), considering the similarity between Zn and Co ion, we referred the [Zn-Al-CO_3] here since their corresponding LDHs structure and XRD pattern is similar.[80]

Table 4.1 compares the propylene/propane separation performances of ZIF-67 membranes grown at different secondary temperatures and times. Though pure in its phase, the membranes

grown at 70°C for 6 h showed a drastic decrease in the C3=/C3 separation factor of 7. This show the membranes have poor grain boundary structure possibly due to the unfavorable growth at relatively low temperature. By extending the reaction time, the propylene/propane separation performances of the ZIF-67 membranes were improved likely due to the improved grain boundary structures as shown in Figure 4.9 and Table 4.1. With a thickness of ~ 500 nm, the membrane grown at 70°C for 2 days showed a propylene/propane separation factor of 67 with a propylene permeance of 273 x 10^{-10} mol/(m^2·pa·s). This turns out to be one of the thinnest ZIF membranes ever reported. Furthermore, this is the first phase-pure ZIF-67 membranes showing propylene/propane separation performances.

Table 4.1 Summary of separation performances for different secondary growth time and temperature

Temperature, SG time	Propylene Permeance (GPU)	Selectivity Factor
90°C, 6 h	79.74	21
80°C, 6 h	47.24	55
70°C, 6 h	69.25±2.62	7±1
70°C, 1 d	70.42±3.82	53.5±6.36
70°C, 2 d	76.82±10.45	68±17.91

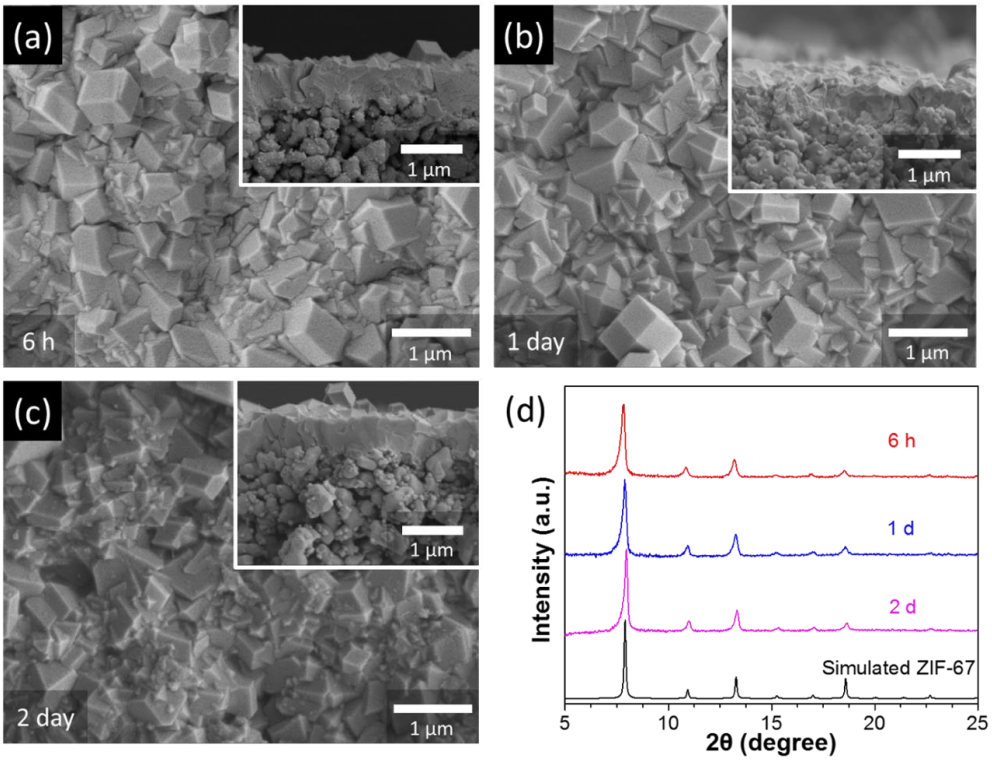

Figure 4.9 SEM images for ZIF-67 membranes after secondary growth at 70°C with the time of (a) 6 h, (b) 1 day, and (c) 2 days as well as (d) their corresponding XRD patterns.

4.2.2 Tertiary growth

Prolonging secondary growth time can effectively heal the defects and provide better grain boundary structure therefore reasonably higher gas separation performances. However after growth time been extend to 3 to 5 days, the resulting membrane was dissolved in the solution with no selectivity, indicating the existence of optimal growth time. After series of repeat experiments, the maximum selectivity around 100 was obtained at 24 hr while the membrane thickness was retained and this appeared to be the best result we could get after SG. Though promising, the ultrathin ZIF-67 membranes failed to show high propylene/propane separation factors as predicted by computational studies.

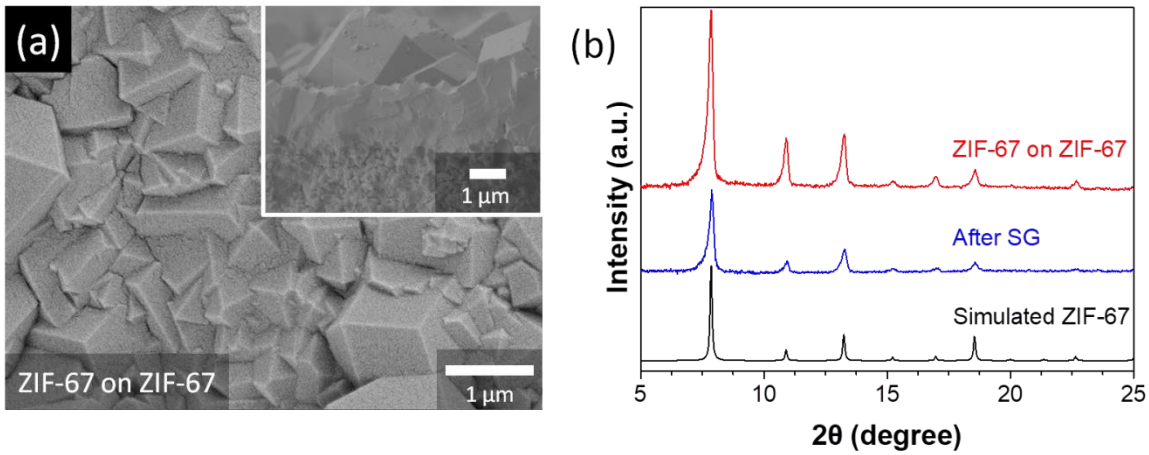

Figure 4.10 (a) SEM images and (b) XRD pattern of the ZIF-67 membrane after tertiary growth.

It is hypothesized that the grain boundary structures of the membranes could be further improved by performing additional growth (i.e. a tertiary growth). Tertiary growth was conducted by repeating the secondary growth upon ZIF-67 membranes synthesized before (70^{o}C, 1 d). As shown in Figure 4.10, the thickness of the membrane (hereafter, TG-ZIF-67 membrane) was increased to 2.5 μm and still phase pure, with a slightly higher (002) peak intensity. The TG-ZIF-67 membrane showed a record-high propylene/propane separation factor of ~ 298 (see Table 4.2). As a comparison, Lee and co-workers [6] estimated the propylene/propane separation factor of 251 using the Maxwell model based on mixed-matrix membrane performances. It should be noted that while preparing this manuscript, it came to our attention that Zhou et al.[78] reported paralyzed ZIF-8 membranes on AAO supports showing extraordinary propylene/propane separation factors of over 300.

Table 4.2 ZIF-67 membranes after combined seeding, SG and then Tertiary growth. Within which 2 out of 4 membranes showed selectivity higher than 50 from the same batch.

Membrane	Sample Code	Propylene Permeance 10^{-10}(mol $m^{-2}s^{-1}Pa^{-1}$)	Propylene Permeance 10^{-10}(mol $m^{-2}s^{-1}Pa^{-1}$)	C3= (GC area)	C3- (GC area)	S.F.
ZIF-67 After TG	182018 - TG-1	81.8	0.27	1941.7	6.5	298
	182018 - TG-3	91.2	0.31	2164.7	7.4	292

4.2.3 The necessity of combined seeding

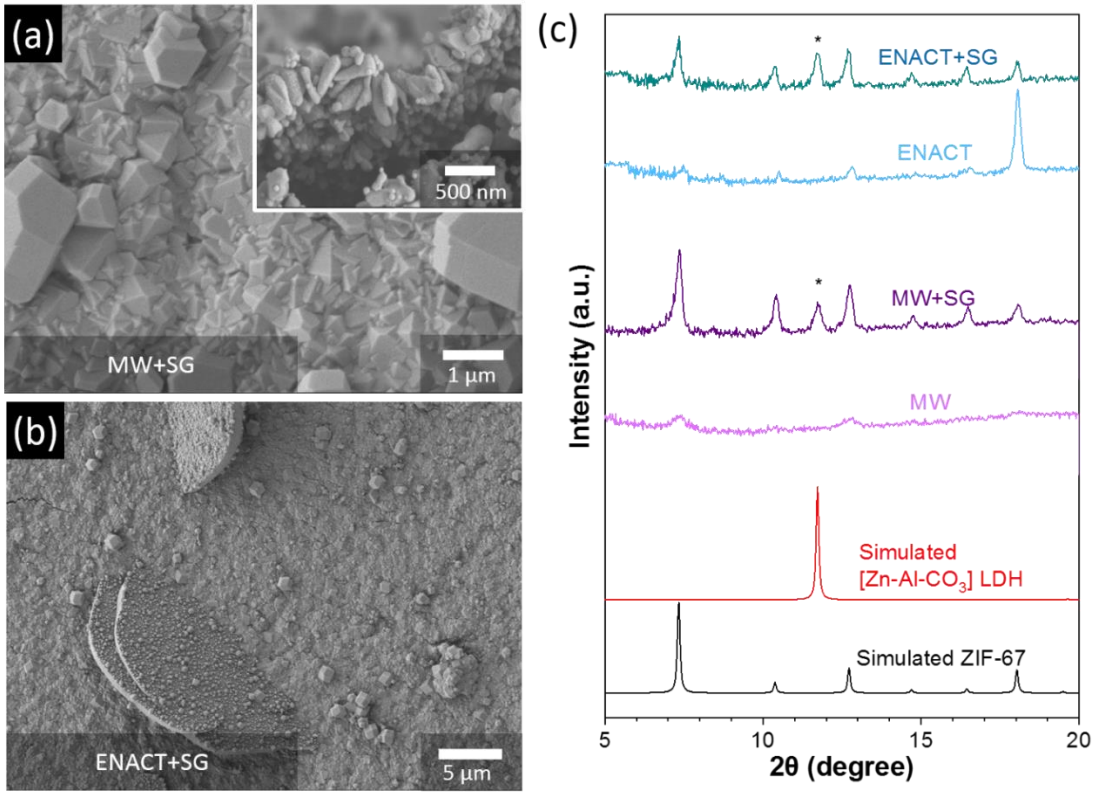

Figure 4.11 SEM images for ZIF-67 membranes after secondary growth with different seeding methods: (a) only microwave seeding, (b) only ENACT seeding and (c) their corresponding XRD patterns. MW stands for microwave seeding here. MW, ENACT, SG stand for microwave seeding, ENACT seeding and secondary growth, respectively.

To examine whether the combined seeding is necessary, secondary growth was conducted for seeded supports by microwave alone (hereafter MW-seeded supports) and those by ENACT alone (hereafter ENACT-seeded supports). As shown in Figure 4.11a, while a continuous layer of ZIF-67 was formed on a MW-seeded support, the ZIF-67 layer was delaminated from the support with most of the crystals showing a shuttle-like shape. This happened possibly due to confined space for densely packed seeds growth therefore the tensile stress developed by the growth of seed crystals would squeeze them into shuttle shape. As the seed crystals deposited on the surface of alumina grains grow, the interstitial spaces are closed by the growing crystals without anchoring underneath, thereby causing tensile stress.

For a support seeded by ENACT alone, however, there were disk-shape particles of layered double hydroxides (LDHs) formed (see Figure 4.11c). Without the anchoring effect provided by MW seeding, the membrane had poor attachment to the support and would crack immediately after been soaked into methanol for wash (Figure 4.12). Kwon et al.[20] observed formation of LDHs when alumina supports were not fully covered with seeds. Al^{3+} ions leached from the alumina support can partially substitute Co^{2+} of $Co(OH)_2$ in the growth solution, forming $[Co\text{-}Al\text{-}CO_3]_{0.33}$ LDHs.[80] The mechanism of LDHs formation has been investigated in details by previous works we discussed before[80, 83, 107]. It was possibly that MW seeding together with ENACT can provide the supports with full coverage, thereby preventing the formation of LDHs. Indeed, phase-pure ZIF-67 membranes were formed as can be seen in Figure 4.6c and 4.8a.

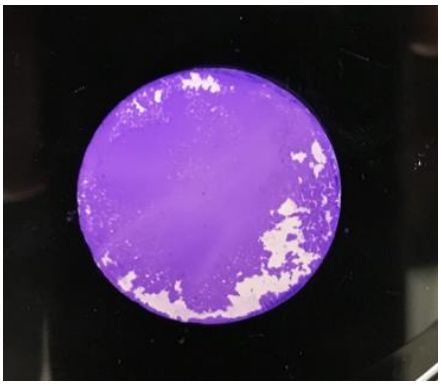

Figure 4.12 Membrane cracking problem caused by poor attachment when seeded by ENACT alone.

4.3 PSLE

The development of high-flux membranes in the propylene/propane separation is one challenging issue centered in the chemical and petrochemical industries, in addition to accompanying the high selectivity has been highly desired. However, it is difficult to achieve by membrane technologies because of their trade-off relation and the similar physicochemical properties of those gases. To improve the propylene permeance, the effective thickness of phase-pure ZIF-67 membranes was further reduced by post-synthetic linker exchange, inspired by previous related works.[72, 101-104] Recently, Jeong et al.[72] reported the modified ZIF-8 membranes (ICA-ZIF-8) by introducing the ICA ligands into the ZIF-8 structure using a PSLE method, exhibiting substantial enhancement in the propylene permeance with excellent preservation of separation factor of ZIF-8. Similarly, we also consider that the newly developed phase-pure ZIF-67 membrane can be modified by ICA using the PSLE method. Furthermore, we expected that the ICA modification of our ZIF-67 membranes can give rise to larger enhancement in permeance than that by the reported ZIF-8 membrane of our group. To this end, we performed the PSLE of the ZIF-67 membranes with ICA second ligands by varying the reaction time for the different ligand exchange conversion.

As shown in Figure 4.13a-b, no significant morphological change or XRD peak position shift was observed as the PSLE carried out by 18 hr. As shown by Jeong et al.,[72] the PSLE of 2-mIm linkers of ZIF-67 membranes with bulkier ICA linkers of ZIF-90 would generally enlarges surface aperture size because of the stretched Co-N bond therefore substantial enhancement in the propylene permeance with preservation of separation factor of the previous structure. Nevertheless, when exchange time been extended to 24 hr or more, we have observed drastic decrease in propylene permeance and selectivity drop (Table 4.3). Even thought the linker exchange ratio was only 11.47%, the membrane structure has already collapsed. From Figure 4.14, the membrane exchanged for 2 days was covered by hollow pores and irregular cracks, the resulting collapse will lead to the blockage of gas transport path therefore low permeance. The crack formation and remaining problems of further PSLE experiment will be discussed in next chapter.

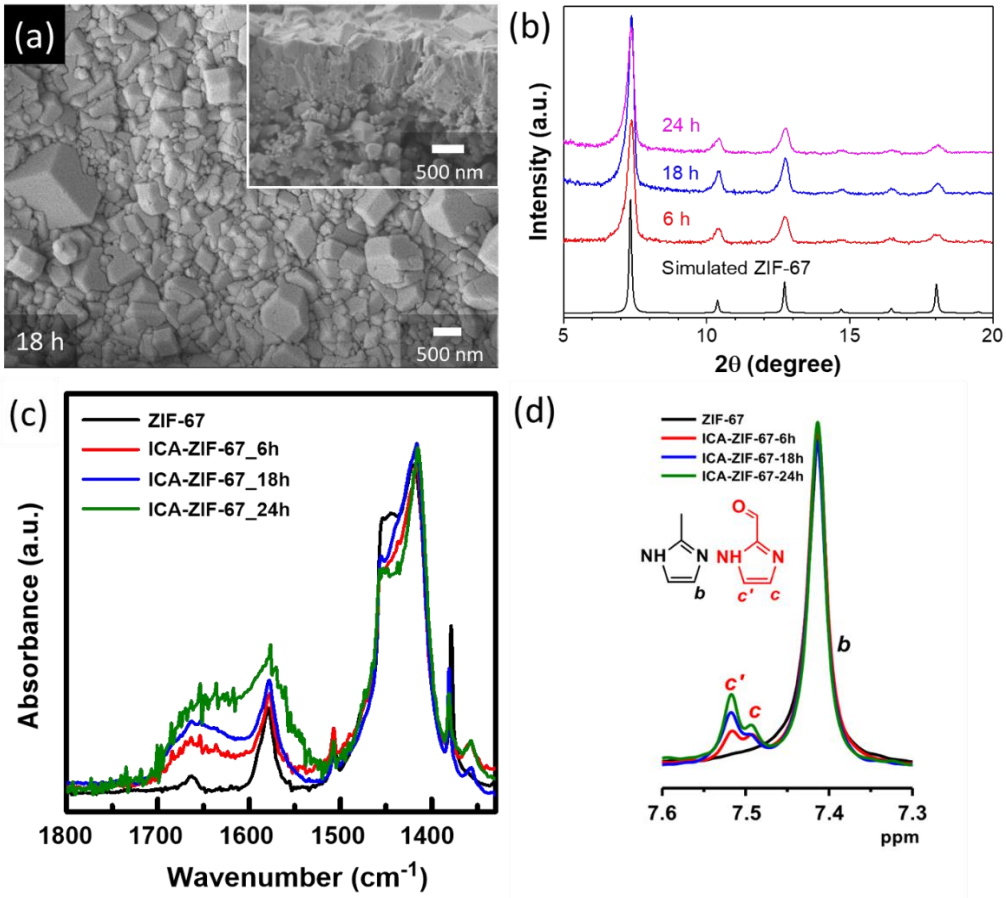

Figure 4.13 (a) SEM images of ZIF-67 membranes after PSLE treatment for different time period 18 h, its corresponding XRD pattern (b). (c) FT-IR and (d) ^{1}H NMR spectra of the ZIF-67 membrane and ICA-modified ZIF-67 (ICA-ZIF-67) membranes with varying the reaction time.^{1}H NMR spectra measured in CD_3OD including 0.02 vol% of H_2SO_4 at room temperature.

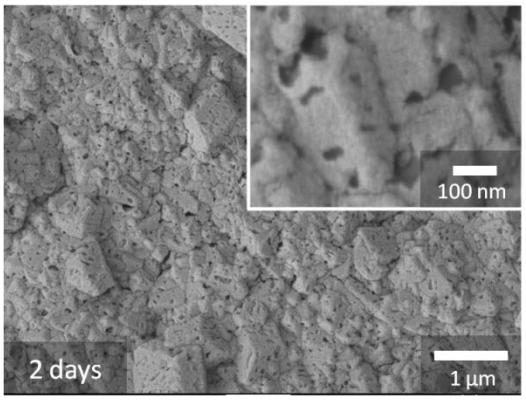

Figure 4.14 SEM images of ZIF-67 membranes after PSLE treatment for 2 days and its zoomed in image (upper right corner).

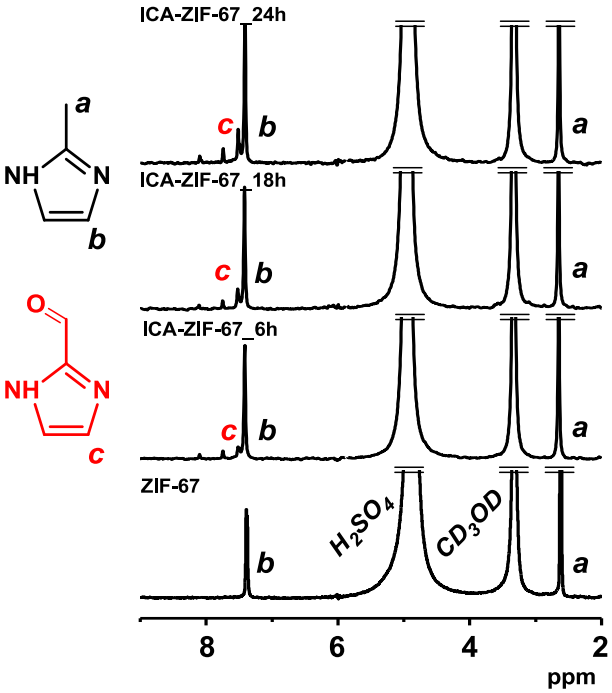

Figure 4.15 ^{1}H NMR Spectra of the ZIF-67 membrane and ICA-modified ZIF-67 membranes with various reaction time.

The acquired ICA-modified ZIF-67 membranes (ICA-ZIF-67, hereafter) were characterized by both FT-IR and NMR (see Figure 4.13). The FT-IR spectrum of ZIF-67 showed three distinctive broad peaks ranging from 1384 to 1600 cm^{-1}, which corresponded to the 2-mIm ligand, which specifically, belong to the C=N stretching modes at 1578 cm^{-1} and the imidazole ring stretching modes at 1450 and 1420 cm^{-1} (see Figure 4.13c). After the PSLE treatment, an increase of aldehyde group contents in the ICA-ZIF-67 membranes was inferred from the smooth growth of the broad peak intensity at 1655 cm^{-1}.[108] To further quantify the ICA content in the ICA-ZIF-67 membranes, we collected the solution ^{1}H NMR spectroscopy (see Figure 4.15), in which ZIF-67 exhibited the two peaks at ca. 2.6 (*a*) and 7.4 (*b*) ppm which corresponded to methyl and methine groups in the mIm ligand, respectively. The introduction of ICA ligand into the ZIF-67 membranes led to the new bimodal peak (*c,c'*) at the more downfield comparing to the peak *b* (See

Figure 4.13d), with corresponds with anticipation because of the electron withdrawing effect of the aldehyde group in ICA.[68] Based on the integration of these separated peaks (*b* and *c,c'*), we calculated the conversion of ICA in ICA-ZIF-67 membranes with different reaction times. As summarized in table 4.3, up to 11.47% of ICA for 24 h PSLE, respectively. As such, both FT-IR and NMR spectrum of ICA-ZIF-67 membranes indicated that the ICA are well introduced to the ZIF-67 membranes by the PSLE method as the secondary ligand.

Table 4.3 ZIF-67 membranes after combined seeding, SG and then PSLE

Temperature, PSLE time	Propylene Permeance (GPU)	Selectivity Factor	Linker exchange ratio
60°C, 6 h	143.65±10.56	15.33±2.08	3.57%
60°C, 18 h	143.15±16.6	11.8±5.94	6.07%
60°C, 24 h	23.25±21.53	6.3±1.84	11.47%

CHAPTER V

CONCLUSIONS AND FUTURE DIRECTIONS

5.1 Conclusions

In summary, we have developed a novel combined seeding method by conjoining well-studied microwave-assisted seeding as well as ENACT seeding and successfully synthesized ultrathin, phase pure ZIF-67 membrane on porous α-Al_2O_3 supports. This is the first phase-pure ZIF-67 membrane reported capable of separating propylene from propane effectively. The resulting ZIF-67 membrane showed a propylene/propane separation factor of 67 and a propylene permeance of ~80 GPUs with a thickness of only 300-500 nm, which can be attributed to several important improvements of our combined seeding technique. The introduction of TEA during microwave seeding step has been proved crucial for reducing the size of seeding crystals. These seeds introduced by microwave seeding fully covered the surface of the support and prevented the formation of $[Co\text{-}Al\text{-}CO_3]_{0.33}$ LDH impurities, while ENACT seeds worked as physical anchor attaching the membrane to the support. In addition, tertiary growth and PSLE experiment based on this ultrathin, phase pure ZIF-67 membrane further improved the selectivity factor to a record high number of 295 and permeance ~298 GPUs, respectively.

5.2 Future work directions

5.2.1 ICA exchange based on TG-ZIF-67 membranes

Compared to previous work related to propylene/propane separation membranes, our membranes have shown its superior performance given its ultra-thin feature. Figure 5.1 has listed related work in Robinson plot with our work marked as red stars. The performances of our

membranes are well above traditional polymer upper bound and locate in commercially attractive zone. By multiple growth and PSLE, the modified membranes are even more competitive among the best propylene/propane separation membranes ever reported as shown in Figure 5.1b. So far, our PSLE experiments have been proved successful based on well-formed SG-ZIF-67 membranes. However when we tried to conduct the same process on TG-ZIF-67 membranes to achieve better selectivity, we have encountered several serious membrane defects.

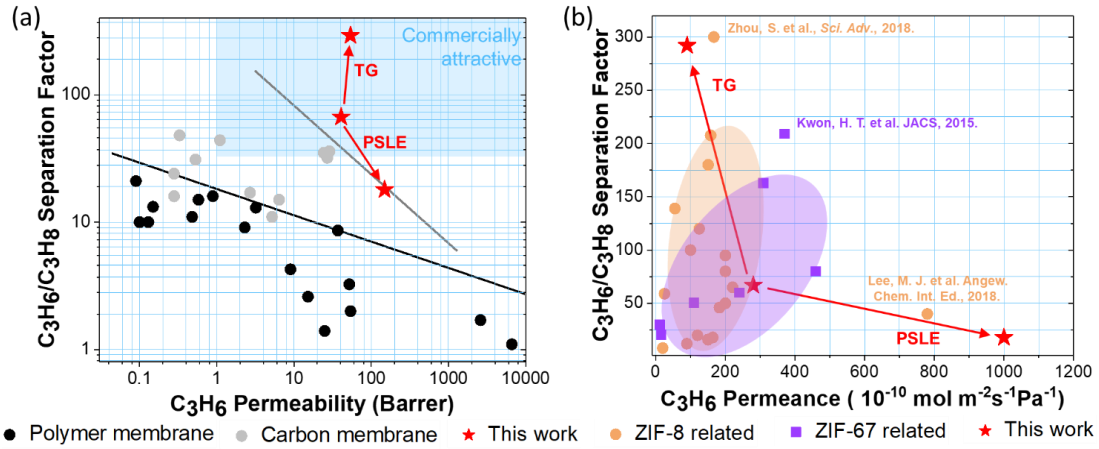

Figure 5.10 Propylene/propane separation performances of our ultrathin, phase-pure ZIF-67 membrane in comparison with previous works. The work by Li, W.B., et al. [77] showing a permeance of ~ 900 GPUs and a selectivity of ~ 70 was not included here.

Under SEM observation, after ICA experiment, several ZIF-67 membranes have shown irregular cracks which is not observed after SG or TG. By taking continuous images as shown in Figure 5.2 at the same spot, we have confirmed that the cracking was caused by intensive energy exerted by electron beam. The cracking formation was significantly accelerated especially when we switched to high magnification which verified our hypothesis. The reason for sample cracking is the aldehyde groups in ICA linkers are much more active and electron beam sensitive compared to mIm. Fortunately the membrane quality was not affected before SEM test.

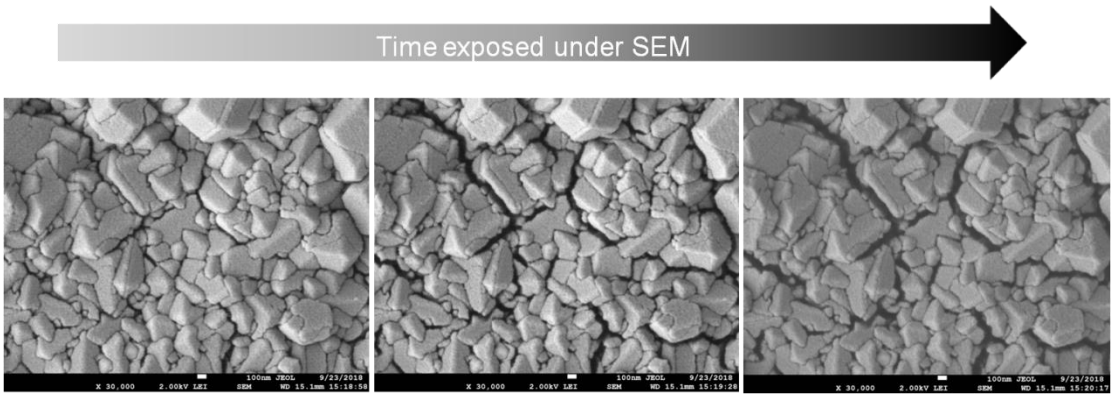

Figure 5.11 The SEM images of ICA exchanged ZIF-67 membrane (TG-ZIF-67) cracking process under electron beam.

A drastic decrease was observed after ICA exchange experiments on TG-ZIF-67 membranes, even when the exchange time was further reduced from 6 hr to 2 hr as shown in Table 5.1. Unlike the results from SG-ZIF-67 membranes, there was no permeance decrease therefore the structure of the membrane should still be intact with no blockage of the gas path. The following SEM pictures (Figure 5.3) have shown a series of bubble-like pores in the middle of the membrane layer, they appeared to be continuous across the whole membrane. It is possible that the interface between the secondary and the tertiary membrane was fragile toward ICA exchange therefore partially collapse may happen when bulkier ICA linkers were introduced which explains why ICA PSLE was not feasible on TG-ZIF-67 membranes.

Table 5.1 Permeation test result after ICA exchanged upon TG-ZIF-67 membranes by exchange time.

Sample code	Propylene Permeance 10^{-10}(mol $m^{-2}s^{-1}Pa^{-1}$)	Propylene Permeance 10^{-10}(mol $m^{-2}s^{-1}Pa^{-1}$)	S.F.
02142019-ZIF67-TG-icaex-6h	1082.92	697.12	2
02142019-ZIF67-TG-icaex-4h	714.91	471.63	2
02142019-ZIF67-TG-icaex-2h	480.95	112.29	4
02142019-ZIF67-TG-icaex-0h	54.88	0.25	221

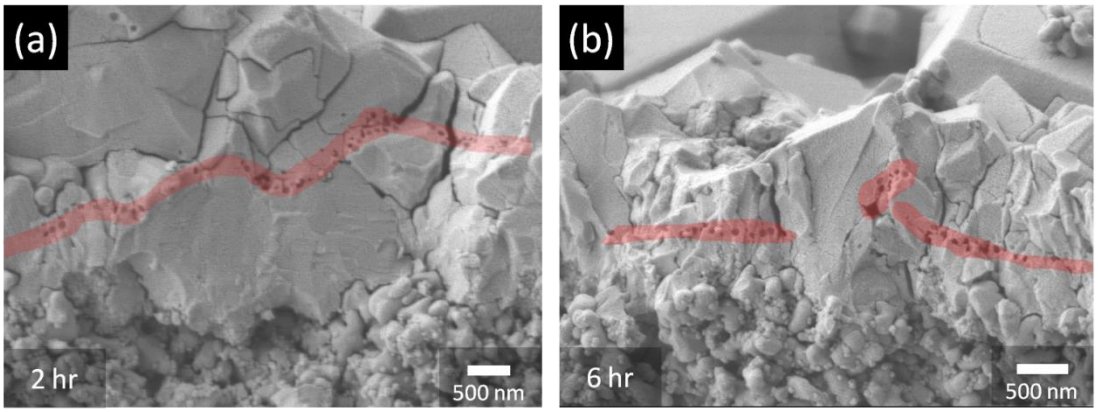

Figure 5.12 The hollow pores area (red highlighted) appeared in TG-ZIF-67 membranes after different ICA exchange time (2 hr, 6 hr).

5.2.2 Atz ligand exchange

By selecting another organic linker 3-amino-1, 2, 4-triazole (Atz hereafter) as PSLE candidate, the ZIF-67 membranes could be modified for CO_2 separation, the Atz-modified ZIF-67 membranes were coded as ZIF67-AM. The acquired ZIF67-AM membranes can substantially enhance CO_2/N_2 and CO_2/CH_4 selectivity since the introduction of amine moieties can enhance chemical interactions with CO_2 while reducing both the surface area and pore volume.[68] As can be seen from Figure 5.4 and Table 5.4 increasing concentration of Atz in the PSLE solution when reaction time fixed at 24 hr will turn the membrane to yellowish and the conversion rate was over 75% even at the lowest Atz concentration. The conversion of Atz was determined by ^1H NMR (0.02 vol% H_2SO_4 in MeOH). Therefore, the desired concentration and reaction time need to be reduced to gain better control toward linker exchange.

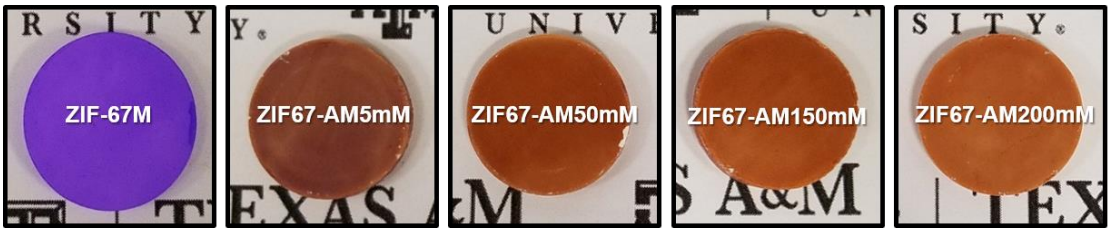

Figure 5.13 The concentration effect of Atz PSLE.

Table 5.2 Profiles of ZIF67-AM membranes synthesized using different Atz concentration

Membrane	Reaction Temperature (°C)	Reaction Time (h)	Atz (mM)	Con (%)
ZIF67-AM5	50	24	5	75.7
ZIF67-AM50	50	24	50	100
ZIF67-AM150	50	24	150	100
ZIF67-AM200	50	24	200	100

5.2.3 Further application

Moreover, since the better control provided by this combined seeding method, the syntheses of other ZIF family ultra-thin membranes have been more accessible. Benefiting from the smoothened surface and more uniformly distributed seed size, we have successfully synthesized ultra-thin ZIF-8 membranes (<500nm) showing great crystallinity and robust structure compared to conventional seeded growth method. Moreover, the combined seeding method may offer a solution in defect-free ZIF-90 membrane fabrication since the cracking problem still exist in relative membrane synthesis. Even though the gas permeation test results have not shown much impressive outcome for other ZIF family members, this universal combined seeding approach has provided enormous potential for future optimization and modification.

REFERENCES

1. Jarvelin, H.; Fair, J. R., Adsorptive Separation of Propylene Propane Mixtures. *Industrial & Engineering Chemistry Research* **1993,** *32* (10), 2201-2207.
2. Jarvelin, H., Separation of Propane and Propylene. *Acta Polytechnica Scandinavica-Chemical Technology Series* **1994,** (222), 1-164.
3. Eldridge, R. B., Olefin Paraffin Separation Technology - a Review. *Industrial & Engineering Chemistry Research* **1993,** *32* (10), 2208-2212.
4. Qiao, Z. H.; Zhao, S.; Sheng, M. L.; Wang, J. X.; Wang, S. C.; Wang, Z.; Zhong, C. L.; Guiver, M. D., Metal-induced ordered microporous polymers for fabricating large-area gas separation membranes. *Nat Mater* **2019,** *18* (2), 163-+.
5. Lin, Y. S., Microporous and dense inorganic membranes: current status and prospective. *Sep Purif Technol* **2001,** *25* (1-3), 39-55.
6. An, H.; Park, S.; Kwon, H. T.; Jeong, H. K.; Lee, J. S., A new superior competitor for exceptional propylene/propane separations: ZIF-67 containing mixed matrix membranes. *Journal of Membrane Science* **2017,** *526*, 367-376.
7. Baker, R. W., Future directions of membrane gas separation technology. *Industrial & Engineering Chemistry Research* **2002,** *41* (6), 1393-1411.
8. Shekhah, O.; Liu, J.; Fischer, R. A.; Woll, C., MOF thin films: existing and future applications. *Chem Soc Rev* **2011,** *40* (2), 1081-1106.
9. Shah, M.; McCarthy, M. C.; Sachdeva, S.; Lee, A. K.; Jeong, H. K., Current Status of Metal-Organic Framework Membranes for Gas Separations: Promises and Challenges. *Industrial & Engineering Chemistry Research* **2012,** *51* (5), 2179-2199.

10. Yaghi, O. M., Reticular Chemistry-Construction, Properties, and Precision Reactions of Frameworks. *J Am Chem Soc* **2016,** *138* (48), 15507-15509.
11. Park, K. S.; Ni, Z.; Cote, A. P.; Choi, J. Y.; Huang, R. D.; Uribe-Romo, F. J.; Chae, H. K.; O'Keeffe, M.; Yaghi, O. M., Exceptional chemical and thermal stability of zeolitic imidazolate frameworks. *Proceedings of the National Academy of Sciences of the United States of America* **2006,** *103* (27), 10186-10191.
12. Bux, H.; Liang, F. Y.; Li, Y. S.; Cravillon, J.; Wiebcke, M.; Caro, J., Zeolitic Imidazolate Framework Membrane with Molecular Sieving Properties by Microwave-Assisted Solvothermal Synthesis. *J Am Chem Soc* **2009,** *131* (44), 16000-+.
13. Pan, Y. C.; Lai, Z. O., Sharp separation of C2/C3 hydrocarbon mixtures by zeolitic imidazolate framework-8 (ZIF-8) membranes synthesized in aqueous solutions. *Chemical Communications* **2011,** *47* (37), 10275-10277.
14. Van Vleet, M. J.; Weng, T. T.; Li, X. Y.; Schmidt, J. R., In Situ, Time-Resolved, and Mechanistic Studies of Metal-Organic Framework Nucleation and Growth. *Chemical Reviews* **2018,** *118* (7), 3681-3721.
15. Zhang, C.; Lively, R. P.; Zhang, K.; Johnson, J. R.; Karvan, O.; Koros, W. J., Unexpected Molecular Sieving Properties of Zeolitic Imidazolate Framework-8. *Journal of Physical Chemistry Letters* **2012,** *3* (16), 2130-2134.
16. Jin, H.; Li, Y. S., Flexibility of metal-organic frameworks for separations: utilization, suppression and regulation. *Current Opinion in Chemical Engineering* **2018,** *20*, 107-113.
17. Lee, M. J.; Kwon, H. T.; Jeong, H. K., Defect-dependent stability of highly propylene-selective zeolitic-imidazolate framework ZIF-8 membranes. *Journal of Membrane Science* **2017,** *529*, 105-113.

18. Krokidas, P.; Castier, M.; Moncho, S.; Sredojevic, D. N.; Brothers, E. N.; Kwon, H. T.; Jeong, H. K.; Lee, J. S.; Economou, I. G., ZIF-67 Framework: A Promising New Candidate for Propylene/Propane Separation. Experimental Data and Molecular Simulations. *J Phys Chem C* **2016,** *120* (15), 8116-8124.
19. Krokidas, P.; Castier, M.; Economou, I. G., Computational Study of ZIF-8 and ZIF-67 Performance for Separation of Gas Mixtures. *J Phys Chem C* **2017,** *121* (33), 17999-18011.
20. Kwon, H. T.; Jeong, H. K.; Lee, A. S.; An, H. S.; Lee, J. S., Heteroepitaxially Grown Zeolitic Imidazolate Framework Membranes with Unprecedented Propylene/Propane Separation Performances. *J Am Chem Soc* **2015,** *137* (38), 12304-12311.
21. Zhou, S.; Wei, Y. Y.; Zhuang, L. B.; Ding, L. X.; Wang, H. H., Introduction of metal precursors by electrodeposition for the in situ growth of metalorganic framework membranes on porous metal substrates. *Journal of Materials Chemistry A* **2017,** *5* (5), 1948-1951.
22. Ruziska, P. A.; Steffens, T. R., On-purpose propylene from olefinic streams. *Proc Ethyl Produc C* **2001,** *10*, 509-517.
23. Hocking, M. B., Petrochemicals. **2005**, 637-668.
24. Plotkin, J. S., The changing dynamics of olefin supply/demand. *Catal Today* **2005,** *106* (1-4), 10-14.
25. Lee, S., **2005**.
26. Ma, X. L.; Williams, S.; Wei, X. T.; Kniep, J.; Lin, Y. S., Propylene/Propane Mixture Separation Characteristics and Stability of Carbon Molecular Sieve Membranes. *Industrial & Engineering Chemistry Research* **2015,** *54* (40), 9824-9831.
27. Grande, C. A.; Cavenati, S.; Da Silva, F. A.; Rodrigues, A. E., Carbon molecular sieves for hydrocarbon separations by adsorption. *Industrial & Engineering Chemistry Research* **2005,**

44 (18), 7218-7227.

28. Ravanchi, M. T.; Kaghazchi, T.; Kargari, A., Application of membrane separation processes in petrochemical industry: a review. *Desalination* **2009,** *235* (1-3), 199-244.
29. Cussler, E. L.; Aris, R.; Bhown, A., On the Limits of Facilitated Diffusion. *Journal of Membrane Science* **1989,** *43* (2-3), 149-164.
30. Howarth, A. J.; Peters, A. W.; Vermeulen, N. A.; Wang, T. C.; Hupp, J. T.; Farha, O. K., Best Practices for the Synthesis, Activation, and Characterization of Metal-Organic Frameworks. *Chem Mater* **2017,** *29* (1), 26-39.
31. Qian, J. F.; Sun, F. A.; Qin, L. Z., Hydrothermal synthesis of zeolitic imidazolate framework-67 (ZIF-67) nanocrystals. *Mater Lett* **2012,** *82*, 220-223.
32. Banerjee, R.; Phan, A.; Wang, B.; Knobler, C.; Furukawa, H.; O'Keeffe, M.; Yaghi, O. M., High-throughput synthesis of zeolitic imidazolate frameworks and application to CO2 capture. *Science* **2008,** *319* (5865), 939-943.
33. Sun, J. Z.; Semenchenko, L.; Lim, W. T.; Rivas, M. F.; Varela-Guerrero, V.; Jeong, H. K., Facile synthesis of Cd-substituted zeolitic-imidazolate framework Cd-ZIF-8 and mixed-metal CdZn-ZIF-8. *Microporous and Mesoporous Materials* **2018,** *264*, 35-42.
34. Zhang, X. P.; Wang, Q. Q.; Li, J.; Huang, L.; Yu, D. B.; Dong, S. J., In situ fabrication of hollow ZnO@NC polyhedra from ZIF-8 for the determination of trace Cd(II). *Analyst* **2018,** *143* (12), 2837-2843.
35. Krokidas, P.; Moncho, S.; Brothers, E. N.; Castier, M.; Economou, I. G., Tailoring the gas separation efficiency of metal organic framework ZIF-8 through metal substitution: a computational study. *Phys Chem Chem Phys* **2018,** *20* (7), 4879-4892.
36. Yao, J. F.; Wang, H. T., Zeolitic imidazolate framework composite membranes and thin films:

synthesis and applications. *Chem Soc Rev* **2014,** *43* (13), 4470-4493.

37. Kaneti, Y. V.; Dutta, S.; Hossain, M. S. A.; Shiddiky, M. J. A.; Tung, K. L.; Shieh, F. K.; Tsung, C. K.; Wu, K. C. W.; Yamauchi, Y., Strategies for Improving the Functionality of Zeolitic Imidazolate Frameworks: Tailoring Nanoarchitectures for Functional Applications. *Adv Mater* **2017,** *29* (38).
38. Bhattacharjee, S.; Jang, M. S.; Kwon, H. J.; Ahn, W. S., Zeolitic Imidazolate Frameworks: Synthesis, Functionalization, and Catalytic/Adsorption Applications. *Catal Surv Asia* **2014,** *18* (4), 101-127.
39. Alezi, D.; Belmabkhout, Y.; Suyetin, M.; Bhatt, P. M.; Weselinski, L. J.; Solovyeva, V.; Adil, K.; Spanopoulos, I.; Trikalitis, P. N.; Emwas, A. H.; Eddaoudi, M., MOF Crystal Chemistry Paving the Way to Gas Storage Needs: Aluminum-Based soc-MOF for CH4, O-2, and CO2 Storage. *J Am Chem Soc* **2015,** *137* (41), 13308-13318.
40. Peng, Y.; Krungleviciute, V.; Eryazici, I.; Hupp, J. T.; Farha, O. K.; Yildirim, T., Methane Storage in Metal-Organic Frameworks: Current Records, Surprise Findings, and Challenges. *J Am Chem Soc* **2013,** *135* (32), 11887-11894.
41. Rodenas, T.; Luz, I.; Prieto, G.; Seoane, B.; Miro, H.; Corma, A.; Kapteijn, F.; Xamena, F. X. L. I.; Gascon, J., Metal-organic framework nanosheets in polymer composite materials for gas separation. *Nat Mater* **2015,** *14* (1), 48-55.
42. Qiu, S. L.; Xue, M.; Zhu, G. S., Metal-organic framework membranes: from synthesis to separation application. *Chem Soc Rev* **2014,** *43* (16), 6116-6140.
43. Horcajada, P.; Chalati, T.; Serre, C.; Gillet, B.; Sebrie, C.; Baati, T.; Eubank, J. F.; Heurtaux, D.; Clayette, P.; Kreuz, C.; Chang, J. S.; Hwang, Y. K.; Marsaud, V.; Bories, P. N.; Cynober, L.; Gil, S.; Ferey, G.; Couvreur, P.; Gref, R., Porous metal-organic-framework nanoscale

carriers as a potential platform for drug delivery and imaging. *Nat Mater* **2010,** *9* (2), 172-178.

44. Horcajada, P.; Serre, C.; Maurin, G.; Ramsahye, N. A.; Balas, F.; Vallet-Regi, M.; Sebban, M.; Taulelle, F.; Ferey, G., Flexible porous metal-organic frameworks for a controlled drug delivery. *J Am Chem Soc* **2008,** *130* (21), 6774-6780.
45. Gascon, J.; Corma, A.; Kapteijn, F.; Xamena, F. X. L. I., Metal Organic Framework Catalysis: Quo vadis? *Acs Catal* **2014,** *4* (2), 361-378.
46. Lee, J.; Farha, O. K.; Roberts, J.; Scheidt, K. A.; Nguyen, S. T.; Hupp, J. T., Metal-organic framework materials as catalysts. *Chem Soc Rev* **2009,** *38* (5), 1450-1459.
47. Wang, L.; Han, Y. Z.; Feng, X.; Zhou, J. W.; Qi, P. F.; Wang, B., Metal-organic frameworks for energy storage: Batteries and supercapacitors. *Coordin Chem Rev* **2016,** *307*, 361-381.
48. Ramaswamy, P.; Wong, N. E.; Shimizu, G. K. H., MOFs as proton conductors - challenges and opportunities. *Chem Soc Rev* **2014,** *43* (16), 5913-5932.
49. Sadakiyo, M.; Yamada, T.; Kitagawa, H., Rational Designs for Highly Proton-Conductive Metal-Organic Frameworks. *J Am Chem Soc* **2009,** *131* (29), 9906-+.
50. Ryder, M. R.; Civalleri, B.; Bennett, T. D.; Henke, S.; Rudic, S.; Cinque, G.; Fernandez-Alonso, F.; Tan, J. C., Identifying the Role of Terahertz Vibrations in Metal-Organic Frameworks: From Gate-Opening Phenomenon to Shear-Driven Structural Destabilization. *Phys Rev Lett* **2014,** *113* (21).
51. Li, Y. S.; Bux, H.; Feldhoff, A.; Li, G. L.; Yang, W. S.; Caro, J., Controllable Synthesis of Metal-Organic Frameworks: From MOF Nanorods to Oriented MOF Membranes. *Adv Mater* **2010,** *22* (30), 3322-+.
52. Liu, Y. Y.; Hu, E. P.; Khan, E. A.; Lai, Z. P., Synthesis and characterization of ZIF-69

membranes and separation for CO2/CO mixture. *Journal of Membrane Science* **2010,** *353* (1-2), 36-40.

53. Hillman, F.; Zimmerman, J. M.; Paek, S.-M.; Hamid, M. R.; Lim, W. T.; Jeong, H.-K., Rapid microwave-assisted synthesis of hybrid zeolitic–imidazolate frameworks with mixed metals and mixed linkers. *Journal of Materials Chemistry A* **2017,** *5* (13), 6090-6099.
54. Khan, M. M.; Shishatskiy, S.; Filiz, V., Mixed Matrix Membranes of Boron Icosahedron and Polymers of Intrinsic Microporosity (PIM-1) for Gas Separation. *Membranes* **2018,** *8* (1).
55. Krokidas, P.; Castier, M.; Moncho, S.; Brothers, E.; Economou, I. G., Molecular Simulation Studies of the Diffusion of Methane, Ethane, Propane, and Propylene in ZIF-8. *J Phys Chem C* **2015,** *119* (48), 27028-27037.
56. Kolokolov, D. I.; Stepanov, A. G.; Jobic, H., Mobility of the 2-Methylimidazolate Linkers in ZIF-8 Probed by H-2 NMR: Saloon Doors for the Guests. *J Phys Chem C* **2015,** *119* (49), 27512-27520.
57. Yeo, Z. Y.; Chai, S. P.; Zhu, P. W.; Mohamed, A. R., An overview: synthesis of thin films/membranes of metal organic frameworks and its gas separation performances. *Rsc Adv* **2014,** *4* (97), 54322-54334.
58. Tanaka, S.; Shimada, T.; Fujita, K.; Miyake, Y.; Kida, K.; Yogo, K.; Denayer, J. M.; Sugita, M.; Takewaki, T., Seeding-free aqueous synthesis of zeolitic imidazolate framework-8 membranes: How to trigger preferential heterogeneous nucleation and membrane growth in aqueous rapid reaction solution. *Journal of Membrane Science* **2014,** *472*, 29-38.
59. Pan, Y. C.; Li, T.; Lestari, G.; Lai, Z. P., Effective separation of propylene/propane binary mixtures by ZIF-8 membranes. *Journal of Membrane Science* **2012,** *390*, 93-98.
60. Kwon, H. T.; Jeong, H. K., In Situ Synthesis of Thin Zeolitic-Imidazolate Framework ZIF-8

Membranes Exhibiting Exceptionally High Propylene/Propane Separation. *J Am Chem Soc* **2013,** *135* (29), 10763-10768.

61. Kwona, H. T.; Jeong, H. K., Improving propylene/propane separation performance of Zeolitic-Imidazolate framework ZIF-8 Membranes. *Chem Eng Sci* **2015,** *124*, 20-26.
62. Butova, V. V.; Budnik, A. P.; Bulanova, E. A.; Soldatov, A. V., New microwave-assisted synthesis of ZIF-8. *Mendeleev Commun* **2016,** *26* (1), 43-44.
63. Xing, T. T.; Lou, Y. B.; Bao, Q. L.; Chen, J. X., Surfactant-assisted synthesis of ZIF-8 nanocrystals in aqueous solution via microwave irradiation. *Crystengcomm* **2014,** *16* (38), 8994-9000.
64. Bao, Q. L.; Lou, Y. B.; Xing, T. T.; Chen, J. X., Rapid synthesis of zeolitic imidazolate framework-8 (ZIF-8) in aqueous solution via microwave irradiation. *Inorg Chem Commun* **2013,** *37*, 170-173.
65. He, G. W.; Babu, D. J.; Agrawal, K. V., Electrophoretic Crystallization of Ultrathin High-performance Metal-organic Framework Membranes. *Jove-Journal of Visualized Experiments* **2018,** (138).
66. Melgar, V. M. A.; Ahn, H.; Kim, J.; Othman, M. R., Highly selective micro-porous ZIF-8 membranes prepared by rapid electrospray deposition. *J Ind Eng Chem* **2015,** *21*, 575-579.
67. Wu, M. A.; Guo, X. F.; Zhao, F. Q.; Zeng, B. Z., A Poly(ethylenglycol) Functionalized ZIF-8 Membrane Prepared by Coordination-Based Post-Synthetic Strategy for the Enhanced Adsorption of Phenolic Endocrine Disruptors from Water. *Sci Rep-Uk* **2017,** *7*.
68. Cho, K. Y.; An, H.; Do, X. H.; Choi, K.; Yoon, H. G.; Jeong, H. K.; Lee, J. S.; Baek, K. Y., Synthesis of amine-functionalized ZIF-8 with 3-amino-1,2,4-triazole by postsynthetic modification for efficient CO2-selective adsorbents and beyond. *Journal of Materials*

Chemistry A **2018,** *6* (39), 18912-18919.

69. Ernst, S., *Advances in Nanoporous Materials*. Elsevier Science: 2009.
70. Shah, M. N.; Gonzalez, M. A.; McCarthy, M. C.; Jeong, H. K., An Unconventional Rapid Synthesis of High Performance Metal-Organic Framework Membranes. *Langmuir* **2013,** *29* (25), 7896-7902.
71. Tsapatsis, M., Toward High-Throughput Zeolite Membranes. *Science* **2011,** *334* (6057), 767-768.
72. Lee, M. J.; Kwon, H. T.; Jeong, H. K., High-Flux Zeolitic Imidazolate Framework Membranes for Propylene/Propane Separation by Postsynthetic Linker Exchange. *Angew Chem Int Edit* **2018,** *57* (1), 156-161.
73. Zhang, S. X.; Wang, Z. G.; Ren, H. T.; Zhang, F.; Jin, J., Nanoporous film-mediated growth of ultrathin and continuous metal-organic framework membranes for high-performance hydrogen separation. *Journal of Materials Chemistry A* **2017,** *5* (5), 1962-1966.
74. He, G. W.; Dakhchoune, M.; Zhao, J.; Huang, S. Q.; Agrawal, K. V., Electrophoretic Nuclei Assembly for Crystallization of High-Performance Membranes on Unmodified Supports. *Adv Funct Mater* **2018,** *28* (20).
75. Hou, J. W.; Sutrisna, P. D.; Zhang, Y. T.; Chen, V., Formation of Ultrathin, Continuous Metal-Organic Framework Membranes on Flexible Polymer Substrates. *Angew Chem Int Edit* **2016,** *55* (12), 3947-3951.
76. Hu, Y. X.; Wei, J.; Liang, Y.; Zhang, H. C.; Zhang, X. W.; Shen, W.; Wang, H. T., Zeolitic Imidazolate Framework/Graphene Oxide Hybrid Nanosheets as Seeds for the Growth of Ultrathin Molecular Sieving Membranes. *Angew Chem Int Edit* **2016,** *55* (6), 2048-2052.
77. Li, W. B.; Su, P. C.; Li, Z. J.; Xu, Z. H.; Wang, F.; Ou, H. S.; Zhang, J. H.; Zhang, G. L.; Zeng,

E., Ultrathin metal-organic framework membrane production by gel-vapour deposition. *Nature Communications* **2017,** *8*.

78. Zhou, S.; Wei, Y.; Li, L.; Duan, Y.; Hou, Q.; Zhang, L.; Ding, L.-X.; Xue, J.; Wang, H.; Caro, J., Paralyzed membrane: Current-driven synthesis of a metal-organic framework with sharpened propene/propane separation. *Science Advances* **2018,** *4* (10).
79. Kwon, H. T.; Jeong, H. K., Highly propylene-selective supported zeolite-imidazolate framework (ZIF-8) membranes synthesized by rapid microwave-assisted seeding and secondary growth. *Chemical Communications* **2013,** *49* (37), 3854-3856.
80. Marappa, S.; Kamath, P. V., Structure of the Carbonate-Intercalated Layered Double Hydroxides: A Reappraisal. *Industrial & Engineering Chemistry Research* **2015,** *54* (44), 11075-11079.
81. Wu, X. Y.; Liu, W.; Wu, H.; Zong, X.; Yang, L. X.; Wu, Y. Z.; Ren, Y. X.; Shi, C. Y.; Wang, S. F.; Jiang, Z. Y., Nanoporous ZIF-67 embedded polymers of intrinsic microporosity membranes with enhanced gas separation performance. *Journal of Membrane Science* **2018,** *548*, 309-318.
82. Nian, P.; Cao, Y.; Li, Y. J.; Zhang, X.; Wang, Y. L.; Liu, H. O.; Zhang, X. F., Preparation of a pure ZIF-67 membrane by self-conversion of cobalt carbonate hydroxide nanowires for H-2 separation. *Crystengcomm* **2018,** *20* (17), 2440-2448.
83. Pei, N. A.; Li, Y. J.; Zhang, X.; Cao, Y.; Liu, H. O.; Zhang, X. F., ZnO Nanorod-Induced Heteroepitaxial Growth of SOD Type Co-Based Zeolitic Imidazolate Framework Membranes for H-2 Separation. *Acs Appl Mater Inter* **2018,** *10* (4), 4151-4160.
84. Wang, C. Q.; Yang, F. Q.; Sheng, L. Q.; Yu, J.; Yao, K. X.; Zhang, L. X.; Pan, Y. C., Zinc-substituted ZIF-67 nanocrystals and polycrystalline membranes for propylene/propane

separation. *Chemical Communications* **2016,** *52* (85), 12578-12581.

85. Knebel, A.; Wulfert-Holzmann, P.; Friebe, S.; Pavel, J.; Strauss, I.; Mundstock, A.; Steinbach, F.; Caro, J., Hierarchical Nanostructures of Metal-Organic Frameworks Applied in Gas Separating ZIF-8-on-ZIF-67 Membranes. *Chem-Eur J* **2018,** *24* (22), 5728-5733.
86. Huang, L.; Zhang, X. P.; Han, Y. J.; Wang, Q. Q.; Fang, Y. X.; Dong, S. J., In situ synthesis of ultrathin metal-organic framework nanosheets: a new method for 2D metal-based nanoporous carbon electrocatalysts. *Journal of Materials Chemistry A* **2017,** *5* (35), 18610-18617.
87. Yoo, Y.; Lai, Z. P.; Jeong, H. K., Fabrication of MOF-5 membranes using microwave-induced rapid seeding and solvothermal secondary growth. *Microporous and Mesoporous Materials* **2009,** *123* (1-3), 100-106.
88. Isaeva, V. I.; Barkova, M. I.; Kustov, L. M.; Syrtsova, D. A.; Efimova, E. A.; Teplyakov, V. V., In situ synthesis of novel ZIF-8 membranes on polymeric and inorganic supports. *Journal of Materials Chemistry A* **2015,** *3* (14), 7469-7476.
89. Hillman, F.; Zimmerman, J. M.; Paek, S. M.; Hamid, M. R. A.; Lim, W. T.; Jeong, H. K., Rapid microwave-assisted synthesis of hybrid zeolitic-imidazolate frameworks with mixed metals and mixed linkers. *Journal of Materials Chemistry A* **2017,** *5* (13), 6090-6099.
90. Yang, L. S.; Lu, H. M., Microwave-assisted Ionothermal Synthesis and Characterization of Zeolitic Imidazolate Framework-8. *Chinese Journal of Chemistry* **2012,** *30* (5), 1040-1044.
91. Yoo, Y.; Jeong, H.-K., Rapid fabrication of metal organic framework thin films using microwave-induced thermal deposition. *Chemical communications* **2008,** (21), 2441-2443.
92. Marti, A. M.; Van, M.; Balkus, K. J., Tuning the crystal size and morphology of the substituted imidazole material, SIM-1. *Journal of Porous Materials* **2014,** *21* (6), 889-902.
93. Nordin, N. A. H. M.; Ismail, A. F.; Mustafa, A.; Goh, P. S.; Rana, D.; Matsuura, T., Aqueous

room temperature synthesis of zeolitic imidazole framework 8 (ZIF-8) with various concentrations of triethylamine. *Rsc Adv* **2014,** *4* (63), 33292-33300.

94. Xin, Z. F.; Chen, X. S.; Wang, Q.; Chen, Q.; Zhang, Q. F., Nanopolyhedrons and mesoporous supra-structures of Zeolitic Imidazolate framework with high adsorption performance. *Microporous and Mesoporous Materials* **2013,** *169*, 218-221.
95. Liguori, P. F.; Russo, B.; Melicchio, A.; Golemme, G., Synthesis and gas sorption behaviour of ZIF-90 with large pore volume. *New Journal of Chemistry* **2017,** *41* (22), 13235-13239.
96. Zhang, W.; Jiang, X. F.; Wang, X. B.; Kaneti, Y. V.; Chen, Y. X.; Liu, J.; Jiang, J. S.; Yamauchi, Y.; Hu, M., Spontaneous Weaving of Graphitic Carbon Networks Synthesized by Pyrolysis of ZIF-67 Crystals. *Angew Chem Int Edit* **2017,** *56* (29), 8435-8440.
97. Wang, S. X.; Lv, Y.; Yao, Y. J.; Yu, H. J.; Lu, G., Modulated synthesis of monodisperse MOF-5 crystals with tunable sizes and shapes. *Inorg Chem Commun* **2018,** *93*, 56-60.
98. Yang, J. M.; Qi, Z. P.; Kang, Y. S.; Liu, Q.; Sun, W. Y., Effect of additives on morphology and size and gas adsorption of SUMOF-3 microcrystals. *Microporous and Mesoporous Materials* **2016,** *222*, 27-32.
99. Wang, Z. Q.; Cohen, S. M., Postsynthetic modification of metal-organic frameworks. *Chem Soc Rev* **2009,** *38* (5), 1315-1329.
100. Han, S. H.; Kwon, H. J.; Kim, K. Y.; Seong, J. G.; Park, C. H.; Kim, S.; Doherty, C. M.; Thornton, A. W.; Hill, A. J.; Lozano, A. E.; Berchtoldf, K. A.; Lee, Y. M., Tuning microcavities in thermally rearranged polymer membranes for CO2 capture. *Phys Chem Chem Phys* **2012,** *14* (13), 4365-4373.
101. Fei, H. H.; Cahill, J. F.; Prather, K. A.; Cohen, S. M., Tandem Postsynthetic Metal Ion and Ligand Exchange in Zeolitic Imidazolate Frameworks. *Inorg Chem* **2013,** *52* (7), 4011-4016.

102. Takaishi, S.; DeMarco, E. J.; Pellin, M. J.; Farha, O. K.; Hupp, J. T., Solvent-assisted linker exchange (SALE) and post-assembly metallation in porphyrinic metal-organic framework materials. *Chem Sci* **2013,** *4* (4), 1509-1513.

103. Erkartal, M.; Erkilic, U.; Tam, B.; Usta, H.; Yazaydin, O.; Hupp, J. T.; Farha, O. K.; Sen, U., From 2-methylimidazole to 1,2,3-triazole: a topological transformation of ZIF-8 and ZIF-67 by post-synthetic modification. *Chemical Communications* **2017,** *53* (12), 2028-2031.

104. Byers, J.; Tsung, C. K.; Morabito, J.; Li, Z. H.; Kyada, R.; Nero, M., Mechanistic features of linker exchange in ZIF-8 and UiO-66. *Abstr Pap Am Chem S* **2015,** *250*.

105. Kwon, H. T.; Jeong, H. K.; Lee, A. S.; An, H. S.; Lee, T.; Jang, E.; Lee, J. S.; Choi, J., Defect-induced ripening of zeolitic-imidazolate framework ZIF-8 and its implication to vapor-phase membrane synthesis. *Chemical Communications* **2016,** *52* (78), 11669-11672.

106. Sun, J.; Yu, C.; Jeong, H.-K., Propylene-Selective Thin Zeolitic Imidazolate Framework Membranes on Ceramic Tubes by Microwave Seeding and Solvothermal Secondary Growth. *Crystals* **2018,** *8* (10), 373.

107. Yang, Y. L.; Yan, X. L.; Hu, X. Y.; Feng, R.; Zhou, M.; Cui, W. L., Development of zeolitic imidazolate framework-67 functionalized Co-Al LDH for CO2 adsorption. *Colloids and Surfaces a-Physicochemical and Engineering Aspects* **2018,** *552*, 16-23.

108. Shieh, F. K.; Wang, S. C.; Leo, S. Y.; Wu, K. C. W., Water-Based Synthesis of Zeolitic Imidazolate Framework-90 (ZIF-90) with a Controllable Particle Size. *Chem-Eur J* **2013,** *19* (34), 11139-11142.